Received: 22 March 2023 | Revised: 26 May 2023 | Accepted: 21 July 2023

DOI: 10.1002/ecs2.4656

ARTICLE

ECOSPHERE
AN ESA OPEN ACCESS JOURNAL

Increased snow cover enhances gross primary productivity in cold and dry regions of the Tibetan Plateau

Hao Liu[1] | **Pengfeng Xiao**[1,2] | **Xueliang Zhang**[1] | **Youlv Wu**[1]

[1]Jiangsu Provincial Key Laboratory of Geographic Information Science and Technology, Key Laboratory for Land Satellite Remote Sensing Applications of Ministry of Natural Resources, School of Geography and Ocean Science, Nanjing University, Nanjing, Jiangsu, China

[2]Jiangsu Center for Collaborative Innovation in Geographical Information Resource Development and Application, Nanjing, Jiangsu, China

Correspondence
Pengfeng Xiao
Email: xiaopf@nju.edu.cn

Funding information
"GeoX" Interdisciplinary Research Funds for the Frontiers Science Center for Critical Earth Material Cycling, Nanjing University; National Natural Science Foundation of China, Grant/Award Number: 42171307

Handling Editor: Manuel T. Lerdau

Abstract

Snow cover is an important control element in the Tibetan Plateau (TP) ecosystem; however, the impact of snow cover changes on gross primary productivity (GPP) is largely unknown, particularly under complex geographical conditions. In this study, we investigated the impacts of snow cover changes on different seasonal GPP and their mechanisms in different geographical zones using multisource remote sensing data from 1982 to 2018. Snow cover significantly affected GPP by nearly 15% of the TP region, and snow cover days (SCDs) were the dominant snow cover indicators affecting GPP variations compared with snow water equivalent (SWE) and snow cover end date (SCED). In general, an increase in snow cover leads to a significant increase in GPP in regions with low precipitation and temperature, but limits the accumulation of GPP in humid and warm regions. Furthermore, from the humid to the arid zone, the "moisture effect" of snow cover (by altering soil moisture) plays an increasingly important role in regulating GPP variations with increasing drought levels. This study elucidates the importance of snow cover in regulating different seasonal GPP variations and significantly improves our insight into the response of vegetation carbon uptake to snow cover changes in the TP.

KEYWORDS
different geographical zones, gross primary productivity, remote sensing technology, snow cover change, snow ecological processes, Tibetan Plateau

INTRODUCTION

The Tibetan Plateau (TP) ecosystem is a significant part of the terrestrial carbon cycle (Piao et al., 2012) and is highly susceptible to climate change (IPCC, 2021). The warming rate on the TP is almost double that of the global mean warming (Chen et al., 2013; Kuang & Jiao, 2016). Gross primary productivity (GPP) changes are one of the most important climate-induced changes occurring in the TP ecosystem (Ma et al., 2019), reflecting changes in the organic carbon content fixed by green vegetation via photosynthesis and profoundly affecting the carbon balance (Keenan et al., 2013; Xu et al., 2019). As a critical climate driver, snow cover on the TP has experienced dramatic substantial changes over the past 40 years (Smith & Bookhagen, 2018), profoundly affecting vegetation dynamics (Piao et al., 2019; Pulliainen et al., 2017). Thus, investigating the impacts of snow cover changes on GPP is vital for understanding the TP ecosystem response to climate change.

Snow cover can affect vegetation carbon uptake via various physiological and phenological processes, and several studies have documented the significance of different snow cover indicators (Kelsey et al., 2021; Qiu et al., 2019). For example, a thick snow depth in winter can protect soil from low temperatures and decrease root mortality, as observed in snowpack manipulation experiments (Li et al., 2016; Sherwood et al., 2017), which is beneficial for vegetation growth. A high snow water equivalent (SWE) can enhance soil nutrient status and moisture for vegetation growth, ultimately increasing GPP (Knowles et al., 2017; Wipf & Rixen, 2010). In addition, longer snow cover days (SCDs) typically result in a delayed snow cover end date (SCED) and spring vegetation phenology, thereby reducing GPP (Galvagno et al., 2013; Scholz et al., 2018). Different snow cover indicators reflect different characteristics and may have opposite impacts; however, detailed studies comparing their impacts on GPP are lacking.

Recently, some site-scale studies have been performed on a specific vegetation type (Chen et al., 2014) or parts of the TP (Qiu et al., 2019; Wu et al., 2018) to explore snow cover changes affecting GPP or a proxy of GPP (e.g., normalized difference vegetation index [NDVI] and tree ring chronology). However, these findings cannot adequately reflect the situation of the entire TP area. Other studies have investigated vegetation dynamics in response to snow cover changes using remote sensing data over the TP. They have focused on the differences between different geographical environments, such as different river basins (Wan et al., 2014), biomes and climate conditions (Wang, Wu, et al., 2018), and elevation zones (Wang, Fu, et al., 2021). These conclusions are important but not always consistent, such as snow cover changes being significantly (Wang, Wu, et al., 2018) or insignificantly correlated (Wan et al., 2014) with the annual maximum NDVI. In addition, most of the above studies did not exclude the impacts of other climatic indicators (i.e., precipitation, temperature, and short radiation) when investigating snow cover affecting vegetation dynamics, thus failing to fully capture their relationships. Moreover, a legacy effect (several months) of snow cover changes on vegetation growth was observed on the TP (Peng et al., 2010; Wang et al., 2015), demonstrating that snow cover may affect the summer GPP or whole growing season GPP, in addition to the early growing season GPP. However, the responses of different seasonal GPP to snow cover changes remain largely unknown and require further investigation.

Furthermore, the mechanism by which snow cover affects GPP varies geographically, and the effect pathways can be divided into the soil hydrothermal effect (by changing the soil temperature and soil moisture status) and the growth period effect (by changing the vegetation growth period). Previous studies based on experimental or observational data revealed that snow cover affected the early growing season GPP of temperate China (Chen et al., 2019; Wu et al., 2018), the Greater Himalayas, and western North America (Wang, Wang, et al., 2018) primarily by changing soil moisture. Snow cover also affected GPP mainly by altering the spring onset date in Central Europe, boreal regions (Pulliainen et al., 2017), and parts of Alaska (Wang, Wang, et al., 2018); and affected GPP mainly by altering soil temperature in the Arctic regions (Kelsey et al., 2021). However, compared with other regions, there are few studies on the main ecological pathways (the above three effects) of snow cover affecting GPP. It remains unclear how these effects interact to control the GPP–snow relationship, especially under the complex geographical conditions of the TP. This greatly limits our in-depth understanding of the snow cover changes that affect GPP.

In this study, we aimed to investigate snow cover changes affecting different seasonal GPP of the TP using multisource remote sensing data from 1982 to 2018. Specifically, the following three questions were addressed: (1) How do different seasonal GPP (i.e., spring GPP, summer GPP, and whole growing season GPP) respond to snow cover changes in different geographical zones and hydrothermal conditions? (2) What are the dominant snow cover indicators (i.e., SWE, SCD, and SCED) affecting GPP variability and its variations with geographical features? (3) What is the mechanism behind the response differences between snow cover and different seasonal GPP? These results are expected to provide a comprehensive understanding of the different snow cover indicators affecting GPP and implications for improving the terrestrial carbon cycle model that considers snow cover on the TP.

MATERIALS AND METHODS

Study area

The average altitude of the TP (25°59′–40°00′ N, 73°20′–104°47′ E) is more than 4 km, covering an area of approximately 2.5×10^6 km^2, which is the highest plateau on Earth (Figure 1a). The climate of the TP is characterized by significant regional differences in precipitation, strong solar radiation, and low annual mean air temperature (AMT), which are influenced by its low latitude, high elevation, and Indian Ocean monsoon (Chen et al., 2015; Wang, Wu, et al., 2018), and the hydrothermal conditions follow a gradient from northwest to southeast (Figure 1b,c). The snow period on the TP is from September to April of the following year, and the mean annual snow cover extent (SCE) accounts for 16% of the entire area (Shen et al., 2015), which serves as a vital

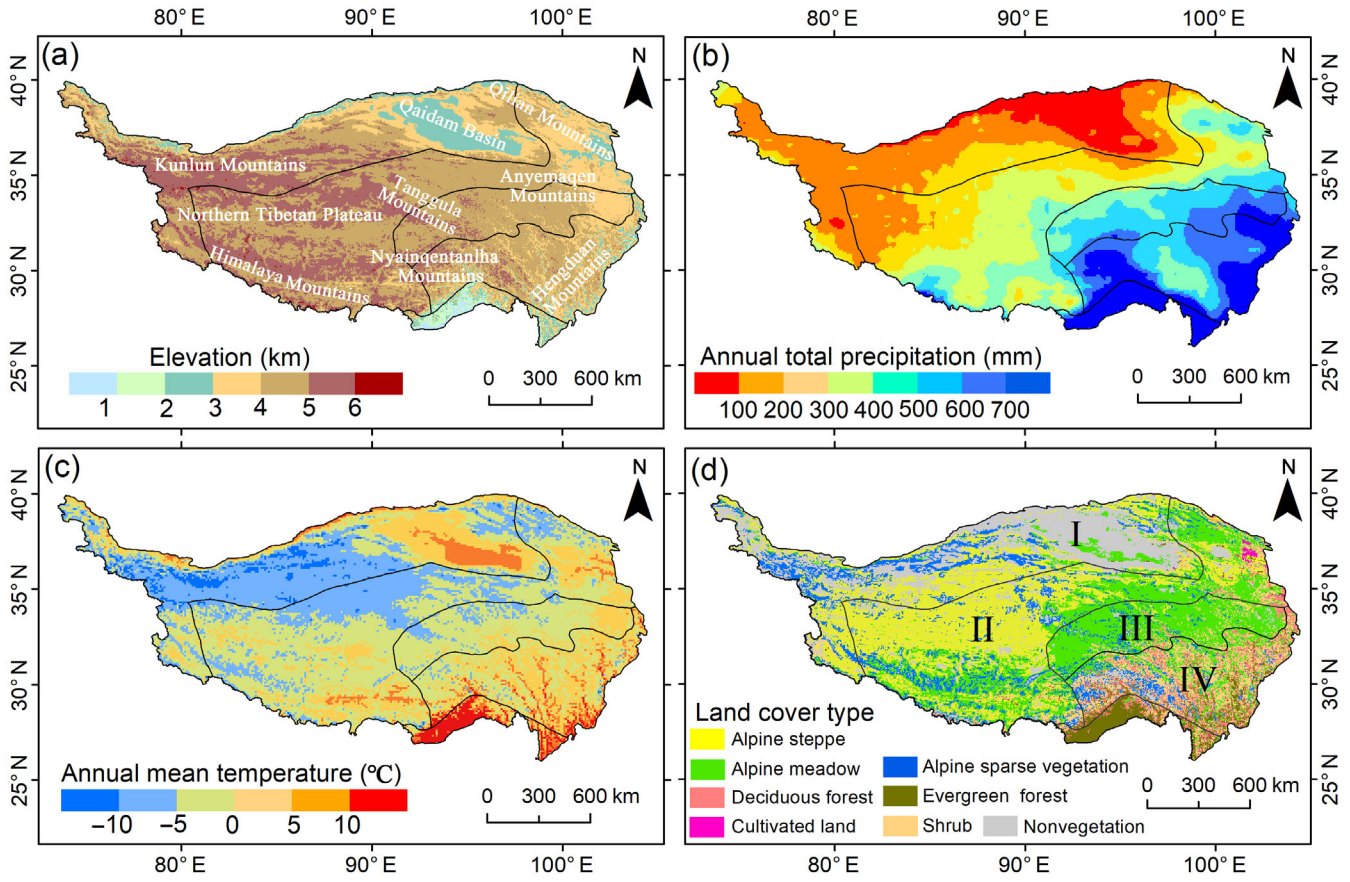

FIGURE 1 Description of the study area. (a) Elevation and topography, (b) annual total precipitation during 1982–2018, (c) annual mean air temperature during 1982–2018, and (d) land cover types and geographical zones, including the arid (I), semiarid (II), subhumid (III), and humid (IV) zones.

freshwater source and is crucial to ecological and hydrological processes (Yao et al., 2019).

The distribution of vegetation on the TP generally follows hydrothermal gradients, showing a gradual transition from coniferous forests, shrubs, and alpine meadows to alpine steppes and deserts (Figure 1d). Alpine meadows and steppes are the two main grassland types, accounting for more than 50% of the entire vegetation area (Dong et al., 2020). Furthermore, considering the unique geographical environment, the TP was divided into four geographical zones (I–IV) to explore snow cover changes that impact GPP variations.

Datasets

Snow cover data

SWE and SCE products were used to obtain three snow cover indicators. The daily SWE product V1.2 was retrieved from the brightness temperature data of the Scanning Multichannel Microwave Radiometer (SMMR), Special Sensor Microwave Imager (SSM/I), and Special Sensor Microwave Imager/Sounder (SSMI/S) sensors using a mixed pixel method (Jiang et al., 2020) and was acquired from the Science Data Bank with a 0.25° × 0.25° grid covering 1980–2020. It provides the most reliable existing and long-term daily SWE data for China and was validated by daily snow depth observations of meteorological stations during the winter of 2011–2019 across the TP, Northeast China, and northern Xinjiang. The SWE product was compared with the meteorological station measurements (155,218 samples) with an unbiased root mean square error of approximately 10 mm, bias values of −1.3 mm, and a correlation coefficient of 0.84 (Jiang et al., 2022).

The long-term daily SCE product V01 was used to extract SCD and SCED data, which were collected from the National TP Data Center. It was produced using Advanced Very High Resolution Radiometer (AVHRR) data via quality control, cloud removal, snow identification, and null filling (Hao et al., 2021), with a 0.05° × 0.05° grid covering 1981–2019. The SCE product has been well validated by ground snow depth

measurements (1,035,546 samples) from China's meteorological stations during the snow seasons of 1981–2019. The SCE product was compared with meteorological station measurements with Cohen's Kappa coefficient and an overall accuracy of 0.72% and 87.4%, respectively, which is the most advanced current AVHRR product.

GPP data

The GPP data were derived from the Global LAnd Surface Satellite (GLASS) AVHRR GPP 8-day product V60 for 1982–2018, with a 0.05° × 0.05° grid. GLASS GPP data were generated using an improved light-use efficiency model and demonstrated high reliability with station observations in various ecosystems (Yuan et al., 2010). Furthermore, compared with the well-known MODIS GPP and FLUXNET GPP products, they have higher temporal resolutions and smoother trajectories (Yu et al., 2018).

Moreover, we estimated the accuracy of GLASS GPP on the TP with three flux tower sites (352 samples were subjected to quality control) obtained from the FLUXNET2015 dataset. Overall, GLASS GPP performs well in capturing the seasonality (correlation coefficient between 0.83 and 0.94) and magnitude (root mean square error [RMSE] between 0.91 and 1.49 g C m^{-2} day^{-1}) of different vegetation GPPs (Figure 2a–c). Meanwhile, the annual variations in GLASS GPP were generally consistent with flux tower measurements (Figure 2e,f). These results reveal that GLASS GPP has high stability and reliability.

Auxiliary data

In addition to snow cover and GPP data, several types of data were used to conduct the mechanism analysis, including soil temperature, soil moisture, and climate data. Soil temperature data were acquired from the ERA5-Land daily product with a 0.1° × 0.1° grid, considering the average of the four soil layers (0–289 cm). The ERA5-Land product is the most advanced reanalysis dataset, which has a long scale and high spatial resolution, and is widely applied in climatic and ecological research (Bastos et al., 2021; Muñoz-Sabater et al., 2021). In addition, several documents revealed that the dataset can capture the spatiotemporal

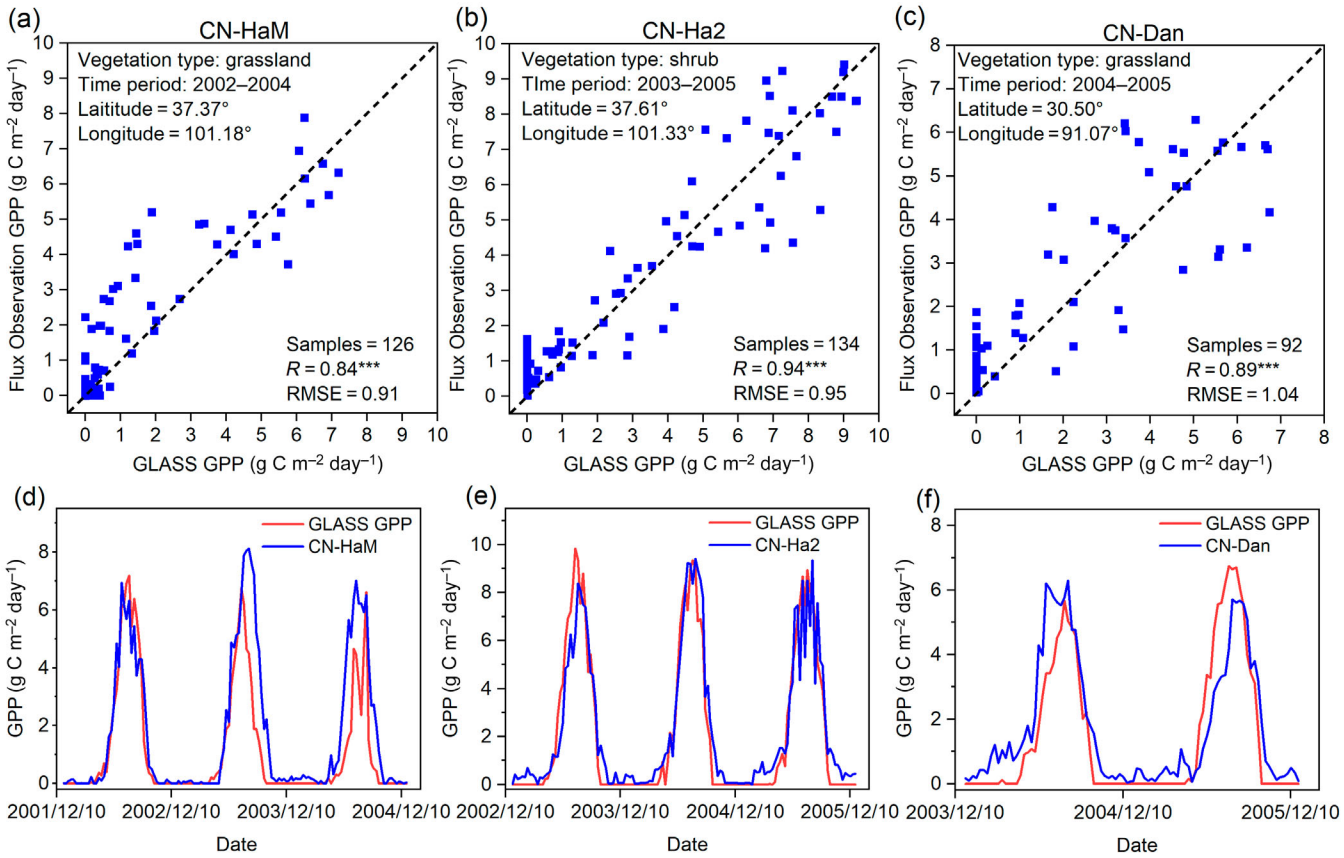

FIGURE 2 Validation of Global LAnd Surface Satellite (GLASS) gross primary productivity (GPP) with three flux tower sites in the Tibetan Plateau. (a–c) The point-based accuracy of GLASS GPP. ***R at a significant level ($p < 0.01$). (d–f) The time series comparison between GLASS GPP and flux tower measurements. RMSE, root mean square error.

pattern of different soil layers of soil temperature across the TP well (Hu et al., 2019; Qin et al., 2017; Yang et al., 2020). For example, one study showed that the daily soil temperature data of different soil layers were consistent with five stations of the TP during 2013–2014, with a mean correlation coefficient and RMSE of nearly 0.9 and 2.87°C, respectively (Yang et al., 2020).

Soil moisture data were derived from the Global Land Evaporation Amsterdam Model (GLEAM) daily root-zone soil moisture dataset v3.5a with a $0.25° \times 0.25°$ grid, which showed good agreement with ground measurements (Martens et al., 2017). For example, the root-zone soil moisture data were generally consistent with four stations during 2015–2016 on the TP, with mean correlation coefficients and bias errors of nearly 0.74 and 0.043 $m^3\ m^{-3}$, respectively, and the accuracy was higher than that of the well-known ESA CCI soil moisture product (Li et al., 2022).

Climate data include temperature, solar radiation, and precipitation data derived from the daily China meteorological forcing dataset (CMFD) V0106 with a $0.1° \times 0.1°$ grid, which has been widely used in the TP because of its high stability and reliability compared with other surface meteorological forcing products (He et al., 2020). The coefficient of determination/mean bias error of temperature, shortwave radiation, and precipitation data of CMFD with reference to China Meteorological Administration observations in the TP are approximately 0.93/0.5°C, 0.8/10 W m^{-2} (He et al., 2020), and 0.88/7.64 mm $month^{-1}$ (Kang et al., 2022), respectively.

Calculation of snow cover and vegetation phenologies

The snow cover phenology indicators include SCD and SCED, which were calculated using the daily AVHRR SCE product. SCD was calculated as the sum of SCDs in a hydrological year (Notarnicola, 2020). To minimize the effect of brief snow cover on SCED, the end date of the last five continuous SCDs observed in a hydrological year was defined as the SCED (Peng et al., 2013; Sun et al., 2020). According to seasonal characteristics of snow cover on the TP (Zhang et al., 2012), the hydrological year was defined as the period from September 1 to August 31 of the following year.

The accuracy of the snow cover phenology algorithm (using the same SCE product) has been well validated in three seasonal snow-covered areas of China using site snow depth data (Hao et al., 2022). The mean absolute error/correlation coefficient of SCD and SCED is approximately 13/0.86 days and 7/0.94 days, respectively, and the accuracy can satisfy the demands of most hydrological and ecological applications. Moreover, we averaged the daily SWE data for the hydrological year to match the SCD and SCED data. Finally, we used snow cover data from 1981 to 2017 to match the GPP data.

To examine the influence of snow cover changes on the vegetation growth period, owing to the time limitations of existing NDVI products (e.g., the longest GIMMS NDVI3g only covers 1982–2015), we used GLASS GPP to extract vegetation phenology features, including the start of the growing season (SOS), end of the growing season (EOS), and length of the growing season (LOS). Specifically, we first reconstructed the time series GPP using a double logistic function, which is a well-validated method (Wang et al., 2019). Before reconstructing the GPP curve, the Savitzky–Golay smoothing method was adopted to filter the outliers to reduce noise (Cao et al., 2018). Second, SOS and EOS were calculated using the mean of the threshold and curvature algorithms based on the fitted daily GPP curve to minimize the uncertainty of SOS and EOS extraction by different methods. For the threshold method, we adopted 10% of the maximum daily GPP per year as the threshold (Wu et al., 2012). In the curvature method, the dates corresponding to the first and last local maximum values of the fitted GPP curve were identified as SOS and EOS, respectively (Zhang et al., 2003). Finally, LOS was defined as the number of days between SOS and EOS.

Methods

Data preprocessing

All datasets covering 1982–2018 were used in this study and interpolated to the same spatial resolution ($0.05° \times 0.05°$) by adopting the nearest neighbor algorithm to match the spatiotemporal resolutions of the GPP data. According to the specific climatic environment and vegetation growth features of the TP (Cong et al., 2017; Yu et al., 2010), spring, summer, and the entire growing season were defined as May–June, July–August, and May–September, respectively, and the mean GPP for each season was calculated for subsequent analysis. Moreover, the nonvegetation, evergreen, and cultivated areas (with no apparent seasonal rhythm) were excluded using a land cover map with a 1:1 million scale (Hou, 2019) before the subsequent analysis.

Trend analysis

The Theil–Sen method (Sen, 1968) was adopted to calculate the slopes between all pairs of points, and the median slope provided the size and sign of the temporal

trend of GPP and snow cover indicators. The trends were calculated by adopting the modified Mann–Kendall test (Hamed & Rao, 1998), which has been widely applied for the evaluation of time series trends because it can solve serial autocorrelation issues and lacks requirements for data distribution. Only pixels with data over 10 years were reserved for trend analysis.

Correlation analysis

Considering the effects of other climatic factors, partial correlation analysis per pixel was applied to investigate the impacts of SCD, SWE, and SCED on different seasonal GPP, removing the impacts of the corresponding period mean air temperature, total precipitation, and mean solar short radiation. Notably, we only focused on the significant correlation pixels ($p < 0.1$), and the comparisons by area were limited to the pixels with significant correlations. Moreover, because the responses of snow cover changes to GPP are highly dependent on the climatic background, we further analyzed their relationships under different air temperatures and precipitation conditions over the TP.

Contribution analysis

Since the correlation among different snow cover indicators, the partial least squares regression (PLSR) analysis was applied to determine the main factors affecting GPP variations for each pixel. PLSR is a powerful method that combines the strengths of multiple linear regression and principal components analysis, avoiding multicollinearity and reflecting the contribution of different snow cover indicators simultaneously, and has been widely applied in ecological studies (Guo et al., 2021; Yu et al., 2010; Zhang et al., 2018). Variable importance on projection (VIP) values were then adopted to reveal the contribution of different snow cover indicators to GPP variations in the PLSR model. Only the importance of different snow cover indicators was examined, and other environmental factors were not considered. The VIP value represents the ability of each snow cover indicator to explain GPP variations, and indicators with a VIP value of more than 1 are considered relatively important (Wold, 1995).

Mechanism analysis

Compared with simple or partial correlation analysis methods, structural equation models can examine complex multivariate relationships among variables and quantify the direct and indirect impacts of explanatory variables on response variables. The partial least squares path model (PLSPM) was used to profile the mechanisms of snow cover impacts on GPP, which is a powerful structural equation model to explore interactive relationships between observed and latent variables and has no requirements for distribution or a large sample size of data (Luo et al., 2017; Sanchez, 2013; Wagg et al., 2014). Based on the empirical relationships among variables (Choler, 2015; Shen et al., 2022; Wang, Wang, et al., 2018), we constructed three pathways to indicate the effect of snow cover on annual GPP variations for different seasons (Figure 3): snow cover → soil temperature → GPP (temperature effect); snow cover → soil moisture → GPP (moisture effect); and snow cover → vegetation phenology → GPP (growth period effect).

Specifically, two latent variables (snow cover and climate) and four observed variables (soil temperature, soil moisture, vegetation growth period, and GPP) were included in PLSPM. For the latent variable "snow cover," three reflective indicators (SCD, SWE, and SCED) were considered. Precipitation, air temperature, and short solar radiation were used to represent the latent variable "climate." For different seasonal GPP, we used different periods of variable data. For example, when exploring the impacts of snow cover on spring GPP/summer GPP/whole growing season GPP, the latent variable "climate," observed variables soil temperature and soil moisture correspond to the same period GPP, and the "vegetation growth period" represents SOS/SOS/LOS.

In the PLSPM analysis, the path coefficients represent the size and direction of the direct effect between two variables. The positive path coefficient indicates that an increase in the explanatory variable leads to an increase in the response variable, and vice versa. The goodness-of-fit index (GOFI) is a global measurement that accounts for path model quality and is used to determine whether the constructed model is effective. A GOFI value higher than 0.36 indicates that the results obtained

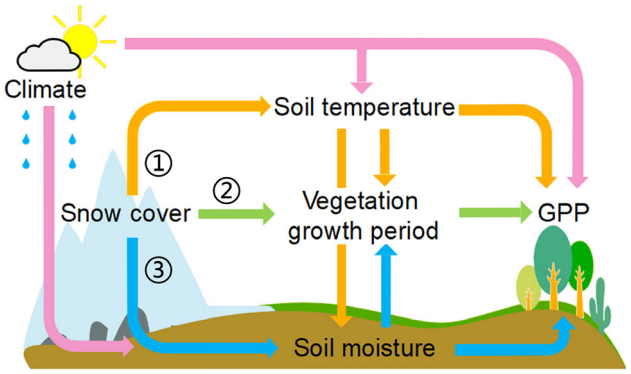

FIGURE 3 Schematic path diagram illustrating the impacts of snow cover on gross primary productivity (GPP).

from the model are reliable (Wetzels et al., 2009). We applied PLSPM to each geographical zone, and all variable data were normalized before path analysis.

RESULTS

Spatiotemporal dynamics of GPP and snow cover

The spatiotemporal dynamics of GPP and snow cover indicators were characterized by their mean values, interannual variations, and trends (Figures 4 and 5). Generally, the mean GPP of different seasons revealed a prominent decrease in the southeast–northwest gradient, which agrees with the spatial distribution of hydrothermal conditions. The annual mean GPPs showed significant increasing trends from 1982 to 2018 for spring, summer, and the whole growing season, where the increasing rate of the total area was up to 0.77, 1.61, and 2.77 g C m^2 $year^{-2}$, respectively. Moreover, GPP in most regions showed an increasing trend during the study period, with regions increasing significantly ($p < 0.1$), accounting for 69%, 65.8%, and 70.8% of spring GPP, summer GPP, and whole growing season GPP, respectively. Meanwhile, the rate of GPP increase in the eastern TP was higher than that in the western TP.

The three snow cover variables showed great spatial heterogeneity across the TP (Figure 5). More specifically, long SCD (>120 days) pixels were mainly concentrated in high mountain regions (e.g., the Kunlun, Nyainqentanglha, and Qilian Mountains). In contrast, short SCD (<30 days) pixels were mainly observed in the Qaidam Basin and the river valleys of the southwestern TP. The annual mean SCD showed a significant decreasing trend, and approximately 40.9% of the pixels had a significant decreasing trend within two days per year. Similar to SCD, SCED also showed a large spatial heterogeneity over the TP, but trends in the annual mean SCED were not statistically significant during the study period. Compared with the interior and eastern regions of the TP, high mountain regions have later SCEDs that occur in May. The regions with significantly advanced SCED occupy approximately 15.7% of the entire region, and these areas are mostly scattered in the Hengduan Mountains, northern areas of the Himalayan Mountains, and the Kunlun Mountains. SWE showed a large interannual fluctuation accompanied by a decreasing trend during 1981–2017, with a decreasing rate of −0.04 mm $year^{-1}$. Approximately 50% of the region had low annual mean SWE values within 10 mm, and regions with high SWE values (>15 mm) were mostly distributed in the Nyenqentangula, Himalayan, and Qilian Mountains. Furthermore, approximately 53% of the regions exhibited a decreasing SWE trend within −0.2 mm $year^{-1}$, with approximately 22% showing a statistically significant decrease.

Responses of GPP to snow cover changes

Relationships between GPP variation and snow cover in different seasons

The correlations between the three snow cover indicators and different seasonal GPP varied significantly in geographical zones (Figure 6). Generally, changes in snow cover have the greatest impact on spring GPP compared with summer GPP and the whole growing season GPP. Specifically, SCD correlated more positively with GPP in all seasons, with a significant positive/negative correlation with GPP in approximately 12.2%/3.4%, 7.6%/7.4%, and 7.9%/6.7% of the entire area, respectively. Spatially, for spring, the pixels with significant positive correlations were mainly found in most areas of the TP, except for the humid zone (IV), while for summer and the whole growing season, they were mostly found in arid (I) and semi-arid (II) zones, and the proportion of positive correlations decreased. The relationship between SWE and GPP showed a similar pattern, and the positive effect of SWE on GPP was mainly distributed in the western TP. Nevertheless, the spatial pattern of the significant correlations between SCED and GPP is relatively scattered. The proportion of significant negative correlations between SCED and spring GPP was higher than that of GPP in summer and the whole growing season, mostly distributed in the western TP.

Relationships between snow cover and GPP under different hydrothermal conditions

Snow cover has a clustering impact on GPP, and their relationships vary significantly over different hydrothermal gradients. According to Figure 7, SCD mostly shows a significant partial positive correlation with spring GPP in regions with −5 to 0°C intervals of AMT and relatively low annual total precipitation (ATP). The positive relationship between SWE and spring GPP showed a similar pattern, and negative relationships occurred mainly in regions with ATP over 500 mm. Furthermore, the linear regression analyses of ATP and AMT indicated a lower regression coefficient (a lower ATP/AMT ratio) for SCD and SWE with significant positive correlations than those with negative correlations, indicating that more snow cover can benefit spring GPP in dry areas with lower ATP. However, significant positive correlations between

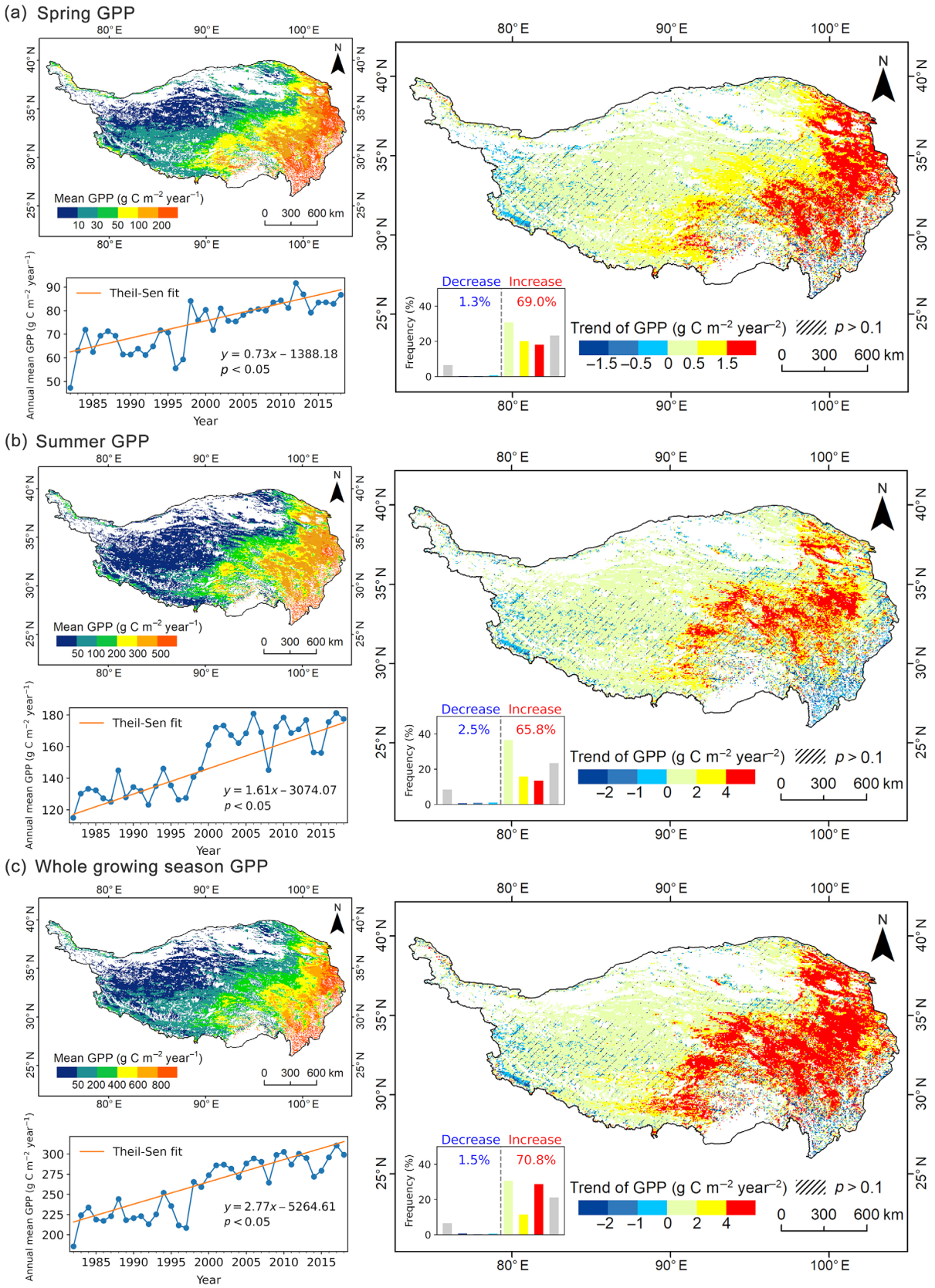

FIGURE 4 Spatial patterns of the interannual variations (lower left), mean values (upper left), and trend of gross primary productivity (GPP) (right) on the Tibetan Plateau during 1982–2018. The inset plots indicate the percentage of the pixels of the GPP trend; colored bars indicate significant GPP changes ($p < 0.1$); gray bars indicate nonsignificant changes. Values in blue and red indicate the sum of significant pixels for decreasing and increasing trends, respectively.

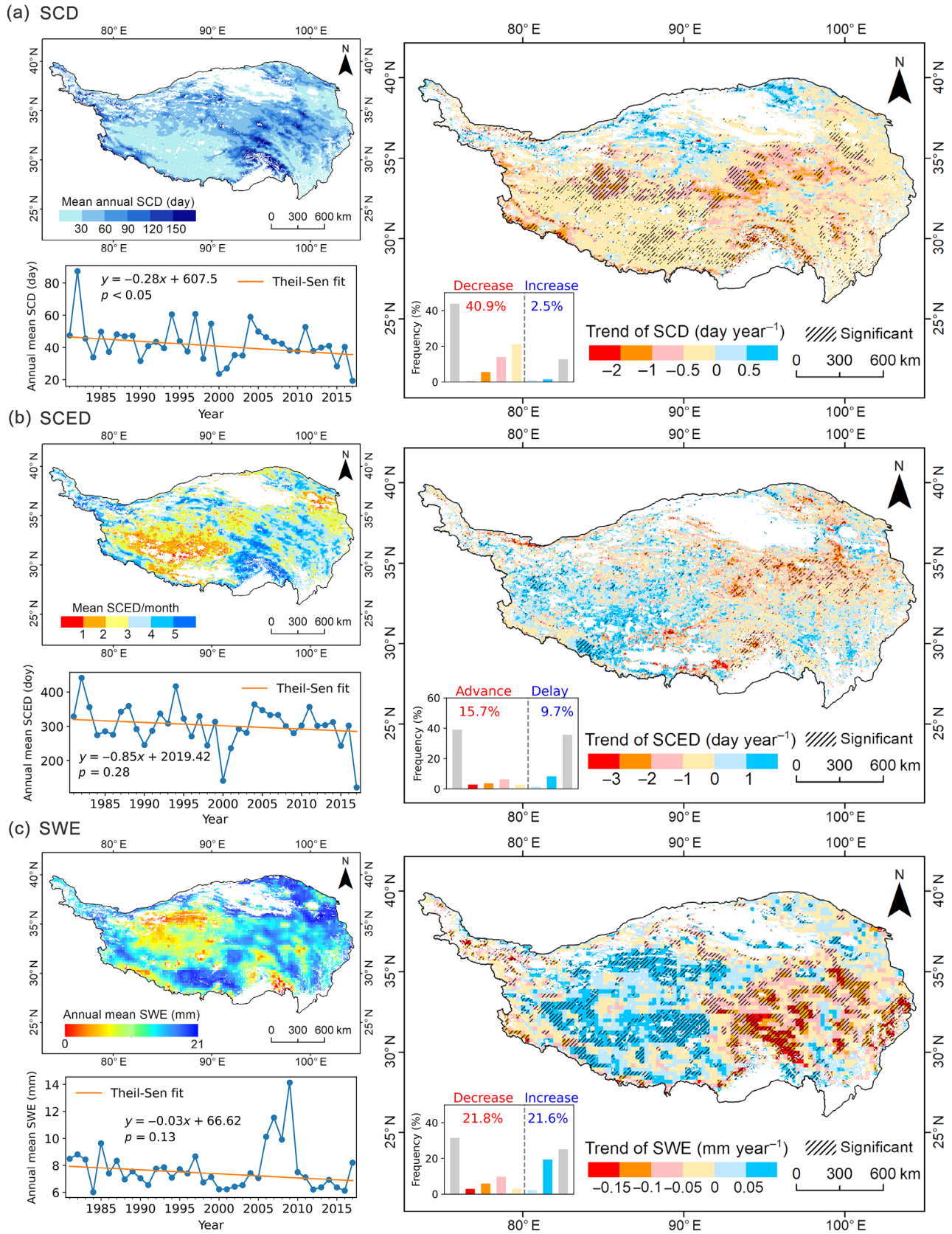

FIGURE 5 Spatial distributions of mean values (upper left), interannual variations (lower left), and trends of three snow cover indicators (right) on the Tibetan Plateau during hydrological years 1981–2017. The inset plots indicate the proportion of the pixels of the snow cover trend; colored bars indicate significant snow cover changes ($p < 0.1$); gray bars indicate nonsignificant changes. Values in blue and red indicate the sum of significant pixels for increasing and decreasing trends, respectively. SCD, snow cover day; SCED, snow cover end date; SWE, snow water equivalent.

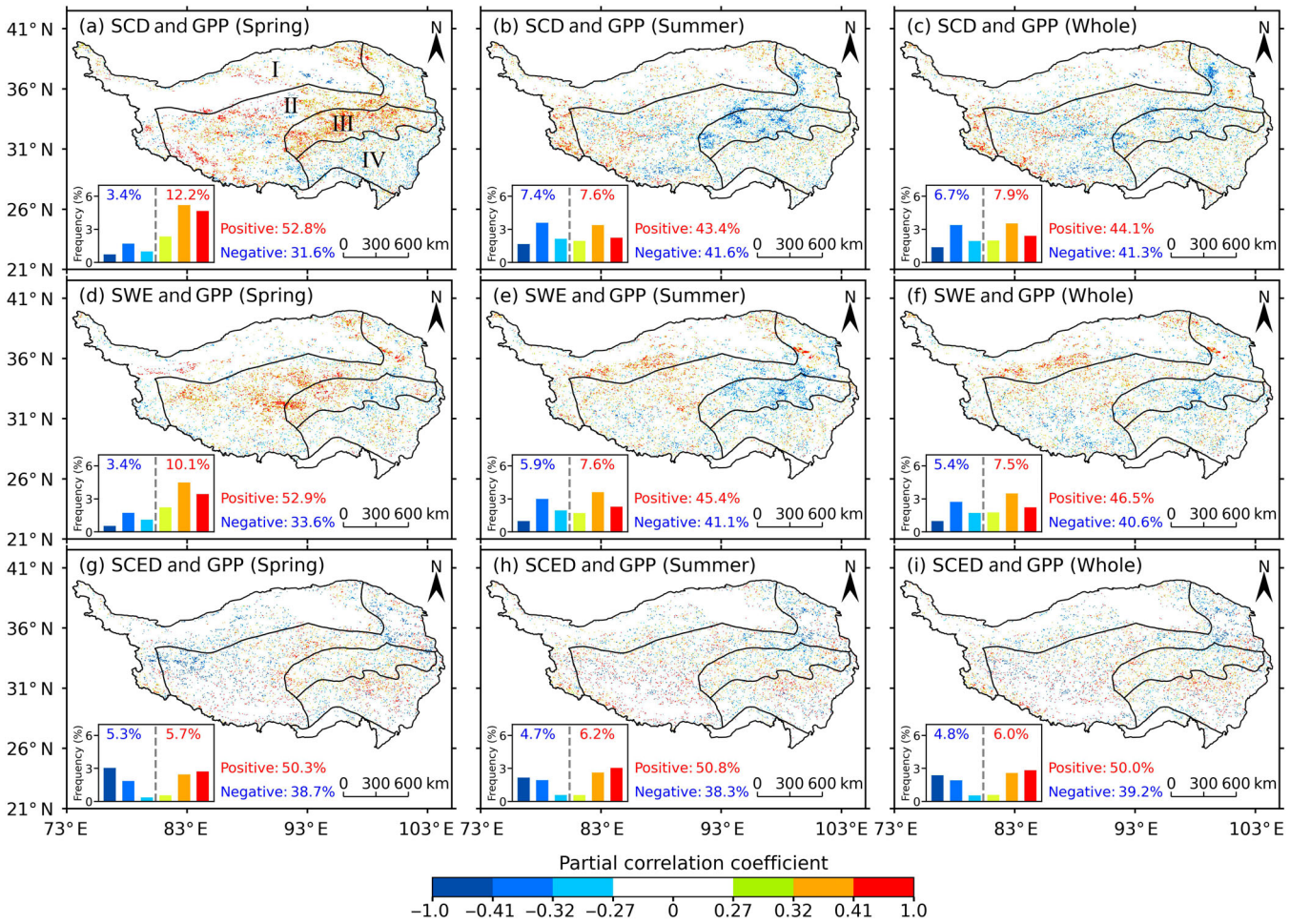

FIGURE 6 Spatial pattern of the responses of different seasonal gross primary productivity (GPP) (spring GPP, summer GPP, and whole growing season GPP) to snow cover changes over different geographical zones during 1982–2018. The colored pixels denote the significant partial correlations at $p < 0.1$, and the absolute value of the significant correlation coefficient exceeds 0.27. Partial correlation coefficients are shown between (a–c) snow cover day (SCD) and GPP, (d–f) snow water equivalent (SWE) and GPP, and (g–i) snow cover end date (SCED) and GPP; values denote the proportion of the insignificant positive and negative pixels. The inset bar plots indicate the proportion of the significant pixels, and values in blue and red indicate the sum of significant negative and positive correlations, respectively.

SCED and spring GPP were primarily concentrated in humid regions with relatively high ATP (>500 mm) and a higher ATP/AMT ratio for SCED, with significant positive and negative correlations with SWE.

In comparison, both summer GPP and whole growing season GPP were significantly positively correlated with SCD and SWE in dry (approximately 250 mm) and cold (AMT < 0°C) regions, and significant negative relationships were primarily concentrated in regions with relatively humid regions (>300 mm). Furthermore, the positive effects of SCD and SWE on GPP tended to increase with decreasing air temperature. Regarding the responses of summer GPP and the whole growing season GPP to SCED, the distribution of the significant positive and negative correlations was scattered, and there was no evident pattern under different hydrothermal conditions. Moreover, the responses of summer GPP and the whole growing season GPP to snow cover changes were similar under the same hydrothermal conditions.

Dominant snow cover indicators affecting the change in GPP

We further identified the snow cover indicators that contributed the most to GPP variability in each pixel based on the importance of the variables in the PLSR model (Figure 8). Among the three snow cover indicators, SCD was the primary explanatory factor for changes in GPP in approximately 37.9% of the whole area, followed by SWE (34.7% on average) and SCED (27.6% on average). The spatial patterns of dominant factors influencing GPP changes showed prominent geographical zones and seasonal differences. More specifically, in summer GPP, the

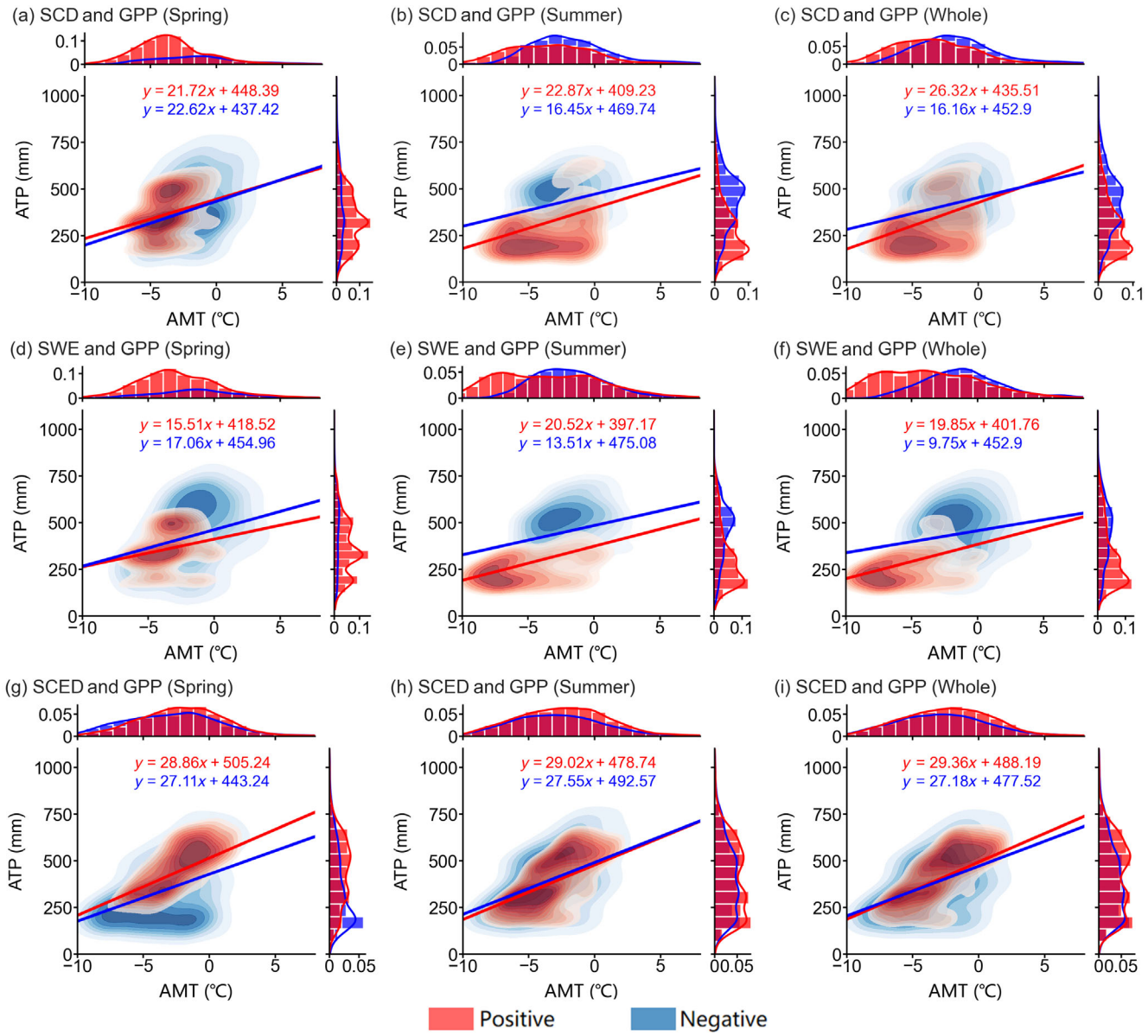

FIGURE 7 Responses of spring gross primary productivity (GPP), summer GPP, and whole growing season GPP to three snow cover indicators with the gradients of annual total precipitation (ATP) and annual mean air temperature (AMT). Significant partial correlation coefficients are shown between (a–c) snow cover day (SCD) and GPP, (d–f) snow water equivalent (SWE) and GPP, and (g–i) snow cover end date (SCED) and GPP, respectively. Only gradients with more than 200 pixels are retained. The top and right histograms of the plot show the distributions of partial correlation coefficients between three snow cover indicators and GPP along the ATP and AMT gradients, and the unit of the *y*-axis is probability. The lines in the plot are derived from linear regression analyses of ATP and AMT, and all regression equations shown are significant.

proportion of SCD-dominated pixels was less than that in spring GPP and the whole growing season GPP, whereas the proportion of SWE-dominated pixels was the opposite. Compared with subhumid (III) and humid (IV) zones, the impacts of SWE were relatively strong in regulating GPP changes in semiarid (II) and arid (I) zones, indicating a greater dependence on obtaining water from snow cover during vegetation carbon uptake in water-limited areas. Moreover, the proportion of pixels dominated by SCED did not show evident differences in summer and the whole growing season of GPP, and the impacts on GPP changes were relatively large in the subhumid (III) and humid (IV) zones.

Mechanisms responsible for the role of snow cover in GPP

Owing to the complex relationship between GPP and snow cover, we profiled the role of each snow cover process affecting different seasonal GPP at the geographical zone scale. Path coefficient diagrams are provided in

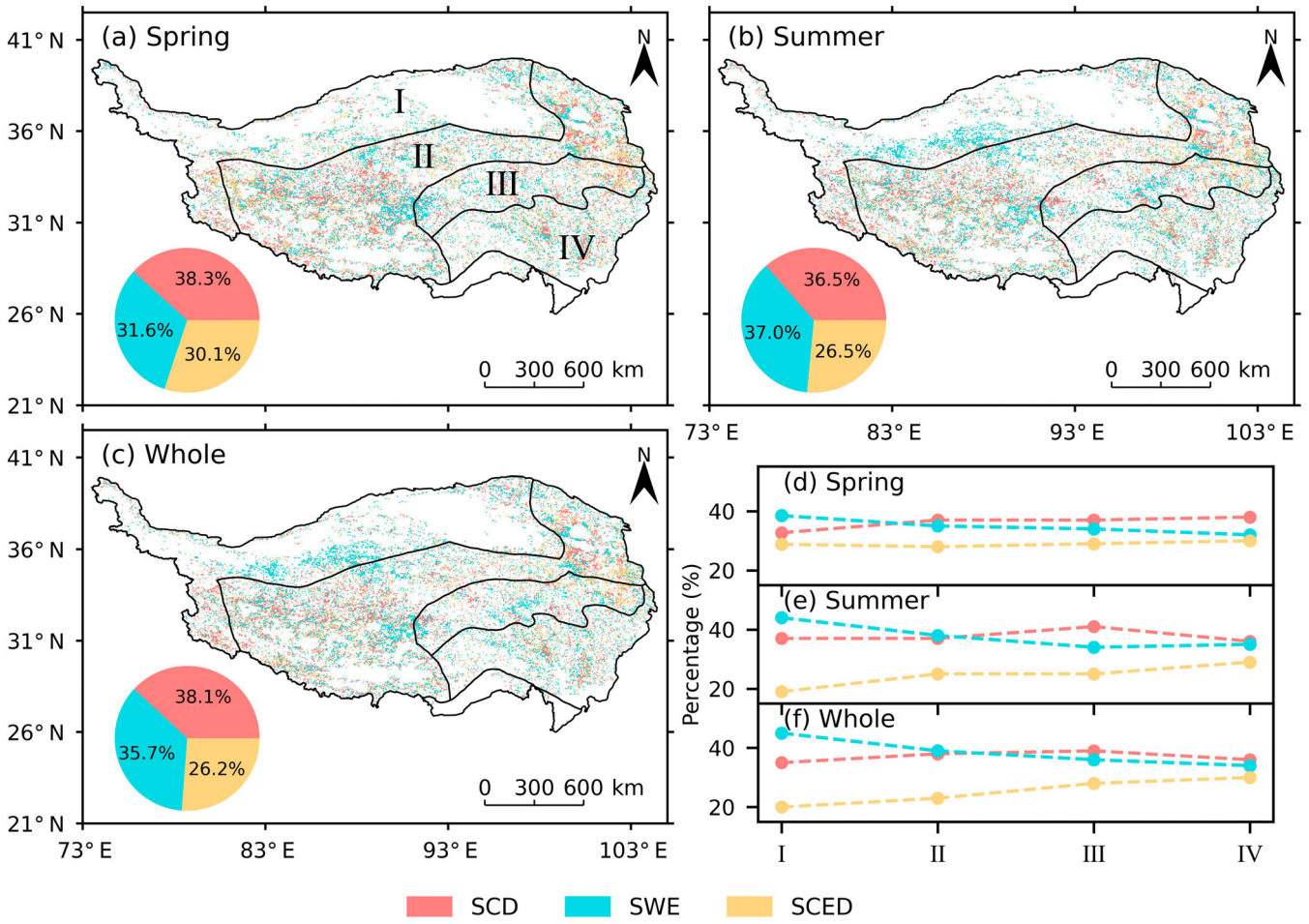

FIGURE 8 Comparison of the dominant snow cover indicators affecting different seasonal gross primary productivity (GPP) changes over the different geographical zones. Spatial distributions of the dominant snow cover indicators affecting GPP variations in (a) spring, (b) summer, and (c) the whole growing season, and the inset plot shows the proportion of each snow cover indicator. (d–f) The proportion of pixels dominated by snow cover indicators in each geographical zone. Only the pixels with variable importance on projection (VIP) > 1 are retained. SCD, snow cover day; SCED, snow cover end date; SWE, snow water equivalent.

Figure 9, and the corresponding direct and indirect effects of snow cover on different factors are shown in Figure 10. The GOFI of all PLSPMs was greater than 0.36, indicating that the established pathway models could well explain GPP variations.

As shown in Figure 9, snow cover has multiple impacts on GPP, varying over different seasons and geographical zones. Specifically, the path coefficient between snow cover and soil temperature (temperature effect) was greater than that of the other two factors, with a direct negative effect of over 0.18 for all geographical zones. For summer and the whole growing season, the negative "temperature effect" of snow cover increased (0.01–0.13) compared with spring across most geographical zones, while the positive "moisture effect" decreased. Furthermore, the "moisture effect" of snow cover increased as the drought level increased, and the total "moisture effect" of snow cover was greater than the "temperature effect" in semiarid and arid zones (Figure 10a–f), leading to a positive effect on GPP. Compared with the "temperature effect" and "moisture effect," the "growth period effect" of snow cover in all growing seasons was relatively weak, with absolute values of the direct effect of 0.01–0.1, which was negative for SOS in all regions and positive for LOS except in the arid zone. In addition to direct effects, snow cover can affect these factors through interactions. For example, snow cover can indirectly affect the vegetation growth period by directly affecting soil moisture and soil temperature, where the indirect effect was quantified as −0.2 in the arid zone (Figure 10c). Moreover, we found that the latent variable "climate" has profound effects on GPP that are partly direct or indirect by changing soil temperatures or soil moisture.

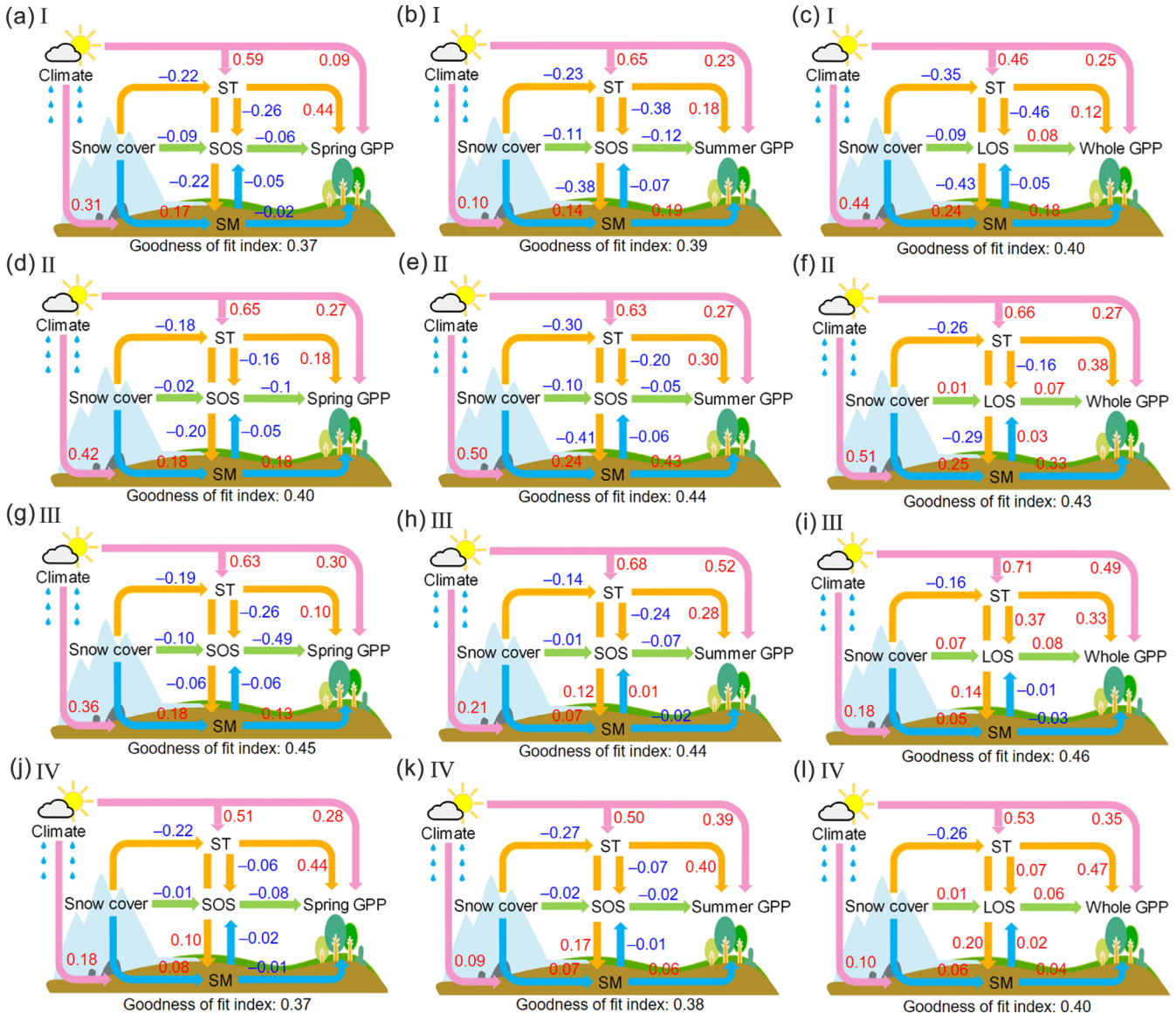

FIGURE 9 Path coefficient diagrams illustrating the effect of snow cover on spring gross primary productivity (GPP) (left column), summer GPP (middle column), and the whole growing season GPP (right column) through the soil temperature, vegetation growth period, and soil moisture over different geographical zones. The values are significant standardized path coefficients ($p < 0.1$) denoting the effect size between factors, where blue and red indicate negative and positive effects, respectively. LOS, length of the growing season; SM, soil moisture; SOS, start of the growing season; ST, soil temperature.

DISCUSSION

Multiple impacts of snow cover on GPP

In this study, we first examined the spatiotemporal patterns of GPP and three snow cover indicators across the TP and found great spatial heterogeneity among all variables (Figures 3 and 4), which was mainly attributed to local geographical conditions. Meanwhile, a large region (over 65% of the study area) has experienced significantly increasing trends of different seasonal GPP and decreasing trends of snow cover over the past four decades, consistent with studies at regional level (Chen et al., 2019) and site level (Wu et al., 2018). Furthermore, although most studies have revealed that air temperature, precipitation, and solar radiation strongly affect GPP (Piao et al., 2012; Wei et al., 2021; Zhang et al., 2020), our findings also demonstrate that significant variations in GPP over a large area of the TP (approximately 15%) are related to snow cover. In addition, a lagged impact of snow cover on the TP was observed, where significant relationships were found in snow cover with summer GPP and the whole growing season GPP, in addition to early growing season GPP.

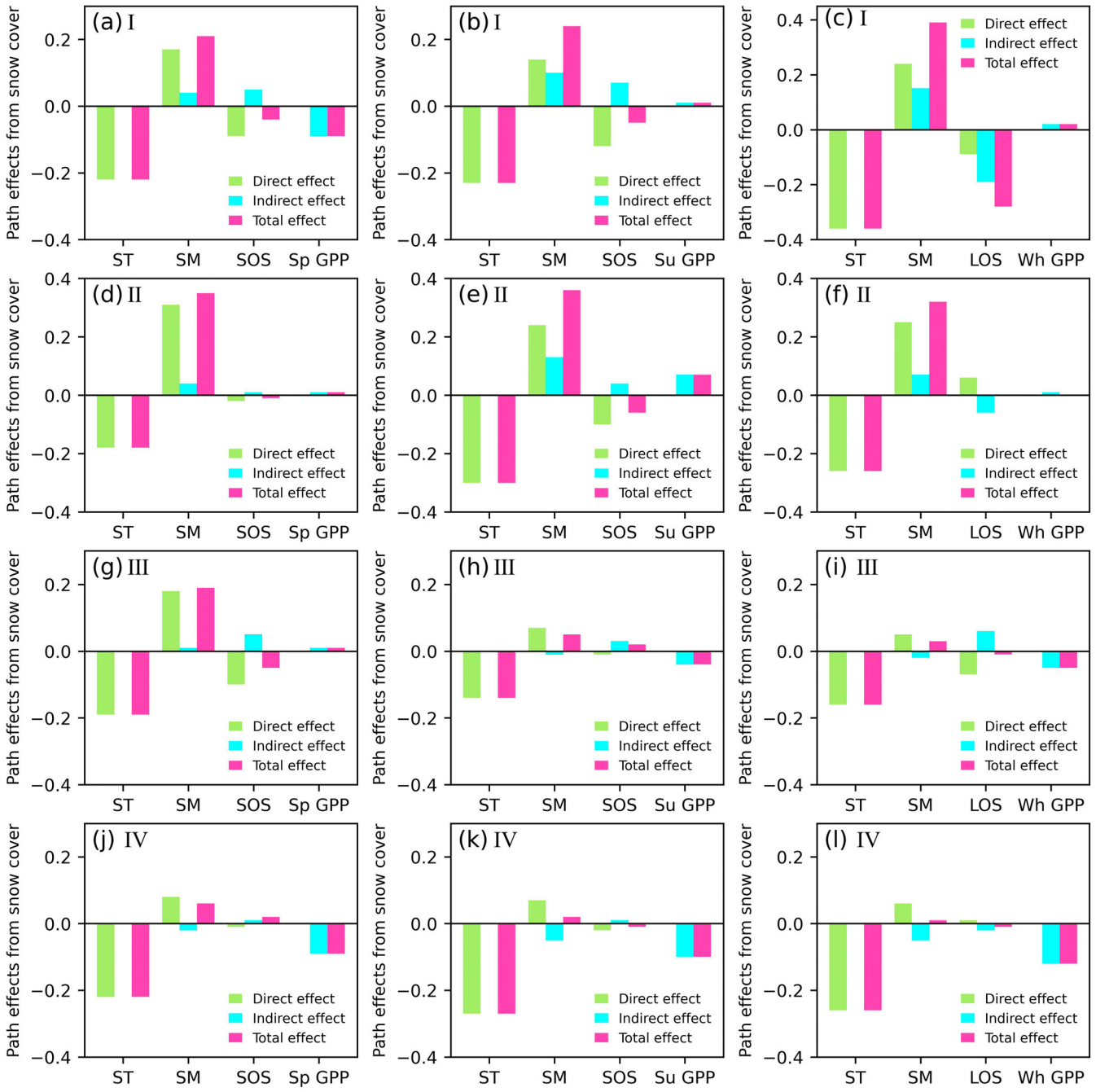

FIGURE 10 Comparison of the direct and indirect effects of snow cover on soil temperature (ST), soil moisture (SM), vegetation growth period (start of the growing season [SOS] or length of the growing season [LOS]), and gross primary productivity (GPP) in spring (Sp GPP), summer (Su GPP), and the whole growing season (Wh GPP) over different geographical zones.

In general, the responses of GPP to snow cover changes were highly related to hydrothermal conditions. We found that snow cover indicators showed significant positive partial correlations with GPP in most regions in all growing seasons (Figures 6 and 7), especially under cold and dry conditions (with ATP < 500 mm and AMT < 0°C), suggesting that increased snow cover was beneficial for the accumulation of GPP. Increased snow cover tends to increase vegetation carbon uptake, as has been documented in many water-limited ecosystems. For example, several short-term snow manipulation experiments of the TP (Chen et al., 2008) and Inner Mongolia (Li et al., 2020) grassland ecosystems showed that increased snow cover was accompanied by increased water available to vegetation, facilitating vegetation growth. Similar results, with growing season vegetation productivity and soil moisture generally increasing in response to greater snow depth, have been

demonstrated by long-term observational studies in temperate China (Chen et al., 2019; Peng et al., 2010). On the other hand, the lower alpine steppe in arid regions may be more completely covered by snow than higher vegetation in humid regions and snow cover can protect low vegetation from low temperatures (Sherwood et al., 2017; Wang, Wu, et al., 2018), which also favors vegetation growth in subsequent seasons. In addition, snow cover positively impacts spring GPP in the subhumid zone (III), whereas it is opposite to the summer GPP and the whole growing season GPP. This is probably because increased snow cover is expected to induce an advanced SOS in these areas, increasing water consumption, possibly causing water stress and constraining GPP accumulation in the late growing seasons (Scholz et al., 2018).

We further identified the dominant snow cover indicators contributing to GPP changes (Figure 8). Compared with the SWE and SCED, SCD was the greatest contributor to GPP changes. This finding is similar to previous studies that demonstrated the prominent impact of SCD on NDVI and vegetation phenology in alpine ecosystems (Qi et al., 2021; Tomaszewska et al., 2020; Wang, Wu, et al., 2018). Moreover, the role of SWE primarily depends on the water conditions of the regions. The seasonal water budget of a region has a closer relationship with SWE compared with other snow cover indicators (You et al., 2020; Zhang & Ma, 2018). The proportion of SCD-dominated pixels for summer GPP decreased compared with spring GPP, whereas the proportion of SWE-dominated pixels increased. The growing season differences can be attributed to the increased water demand for vegetation growth in the peak growing season (Chen et al., 2019), thus showing more sensitivity to SWE. In contrast, the significance of SCED to changes in GPP was relatively small and its spatial distribution was much more fragmented, largely due to the great spatial heterogeneity and instability of snow cover (Tang et al., 2022), coupled with vegetation growth influenced by various non-snow factors on the TP (Piao et al., 2012).

In addition to improving the in-depth understanding of the complex snow–GPP interactions, we provide some implications for improving the terrestrial carbon cycle model based on the above findings. For example, it is essential to consider snow cover effects when using a terrestrial carbon cycle model to simulate GPP variations in seasonally snow-covered areas, and geographical differences must be considered in the modeling settings. Moreover, the snow cover indicators used as inputs for the model can be simplified based on their contributions.

Mechanism differences in different regions

Snow cover showed a high negative "temperature effect" in the subhumid (III) and humid (IV) zones, implying that it has a detrimental impact on GPP accumulation (Figures 9 and 10). Insufficient soil heat isolation in areas with low snow depth and SCDs is one of the reasons behind this negative effect (Wan et al., 2014; Xu et al., 2017). As a result, positive vegetation growth in the following year cannot be ensured due to inadequate soil thermal conditions in these areas. Moreover, a decreasing trend in snow cover during the past four decades (Figure 5) further deteriorated the snow-driven soil temperature supply to promote vegetation growth. Interestingly, compared with snow-free regions, winter soil temperatures tend to be higher in snow-covered regions but are negatively correlated with SCD in the alpine ecosystem during the growing season (Magnani et al., 2017), reducing GPP. This finding explains the result that the eastern regions of the TP have a higher percentage of pixels with negative correlations between SCD and SWE, and GPP during summer and the whole growing season (Figure 6). In water surplus areas, where soil thermal conditions play a critical role in vegetation growth, increased snow cover results in lower growing season soil temperatures and consequently decreased GPP. In contrast, northern Alaska and northern Mongolian Plateau with thick and stable snow cover have positive temperature effects (Chimner et al., 2010; Sa et al., 2021). In these regions, the increase in SCD and snow depth mitigates frost damage to vegetation and increases vegetation carbon uptake.

Moreover, snow cover affecting GPP variation depends mainly on local water conditions. With an increase in drought stress in the region, the positive "moisture effect" of snow cover increases, leading to more pixels with positive correlations between snow cover and GPP, particularly in the middle and late growing seasons. This is mainly attributed to the requirement of hydrothermal conditions for vegetation growth, from thermal to water demand in water-limited areas. In this case, greater snow cover can provide more water resources for vegetation growth and then promote the increase in GPP, consistent with previous results in the alpine ecosystems of the Greater Himalayas (Wang, Wang, et al., 2018) and temperate ecosystems of China (Chen et al., 2019; Peng et al., 2010). However, a positive correlation between snow cover and spring GPP was found in relatively warm and humid areas (subhumid zone), mainly because snow cover leads to earlier SOS, extending the growth period in spring, accompanied by an increase in soil moisture, further enhancing GPP.

Although the close relationship between snowmelt date and SOS has been widely reported (Qi et al., 2021; Sa et al., 2021; Xie et al., 2021), the direct "growth period" effect of snow cover (low path coefficient) appears to be weak in the TP when compared with the "temperature effect" and "moisture effect." This mechanism has also been observed at low latitudes, such as Central Asia and North America (Wang, Wang, et al., 2018). The asynchronous timing of snowmelt and SOS in these regions suggests that additional constraints of environmental factors, such as photoperiod conditions (Wang et al., 2017), soil nutrients (Yano et al., 2015), and permafrost (Wang & Liu, 2022), may weaken the direct association between snow cover and SOS. Furthermore, the two-month difference between snowmelt and SOS (Wang, Wu, et al., 2018) on the TP further supports the view that snow cover mainly influences vegetation phenology through its effect on soil temperature and soil moisture.

Possible snow cover change impacts on future GPP

Our results revealed a significant increase and decrease in different seasonal GPP and snow cover, respectively, across the TP during 1982–2018. However, the positive GPP trend may be constrained against continued global warming. For example, increases in air temperature are generally accompanied by a decrease in snow cover and an increase in vapor pressure deficit, leading to reductions in the available water required for future vegetation growth (Wu et al., 2018). Several previous studies on the TP have reported that snow cover over the 21st century generally decreased under different representative concentration pathway (RCP) scenarios. For example, the trends in annual mean snow depth are approximately $-0.08/-0.11$ cm year^{-1} during 2007–2099 under RCP4.5/8.5 (Wei & Dong, 2015), and the annual mean SCD is shortened by 10–40 days during 2040–2099 under RCP4.5 (Ji & Kang, 2013). GPP in humid regions was more limited by the "temperature effect" of snow cover in the past four decades, and the "moisture effect" assumed an increasingly important role in vegetation carbon uptake with increased drought levels. In this regard, the positive effect of decreased snow cover is expected to gradually aggravate, especially in dry regions, resulting in increased water stress and consequently restraining the accumulation of GPP. With climate warming, we infer that the continuous decrease in snow cover will further reduce GPP in dry and cold regions.

Furthermore, uneven changes in snow cover may aggravate the spatial pattern differences in GPP and further influence the pattern of carbon sinks and sources over the TP. According to the simulation results of the model, under global mean warming of 1.5 and 2°C, the distribution of projected mean SWE indicates an evident west–east gradient with the largest decrease in the western TP, consistent with significant warming in that region (You et al., 2020). Meanwhile, there will be a sharper northwest–southeast wetting gradient over the TP in the future compared with the original distribution of precipitation (Wang, Zhao, et al., 2021). In these circumstances, we infer that the reduction in snow cover weakens its negative "temperature effect" on the wetter eastern TP and further increases GPP. In contrast, the decreased positive "moisture effect" of snow cover that dominates the drier western TP will reduce GPP. Thus, the differences in GPP between the eastern and western TP are anticipated to be further aggravated.

Uncertainties and perspectives

The uncertainties in our results arise from two aspects: the input datasets and the analysis. Specifically, the credibility of our results depends mainly on the quality of the input datasets (e.g., GPP, snow cover, and climate data). Although these datasets demonstrate high reliability with station observations or in situ measurements, they inevitably cause errors when interpolated to the same spatial resolution. Furthermore, for the analysis, we did not consider the impacts of human events, such as human-induced land cover changes (Chen et al., 2013; Liu et al., 2008), stocking rates (Tomaszewska et al., 2020), and pasture maintenance (Zhumanova et al., 2018) on GPP and snow cover dynamics, which may have increased the uncertainties in our findings. Furthermore, the process by which snow cover affects soil nutrients was not involved in the mechanism analysis, mainly because of the shortage of regional-scale soil nutrient data, which limits the knowledge of the mechanisms by which snow cover affects GPP.

Some aspects still require further consideration, such as the responses of GPP to snow cover changes in various elevation zones and vegetation types. Moreover, a combination of long-term in situ observations and higher spatial resolution remote sensing data is required to better explore snow cover changes affecting GPP in the future.

CONCLUSIONS

In this study, we investigated the impact of snow cover on GPP across the TP using multisource remote sensing

data from long-term and large-scale perspectives. Our results revealed that snow cover had significant impacts on spring GPP, summer GPP, and whole growing season GPP across nearly 15%, 13%, and 11% of regions of the TP, respectively, and GPP–snow relationships varied among different snow cover indicators and hydrothermal conditions. SCD was the greatest contributor to GPP variation, followed by SWE and SCED. Strong significant negative relationships were mainly found in humid and cold regions, while significant positive relationships mainly occurred in dry and warm regions and were enhanced with decreasing temperature. Moreover, the "temperature effect" of snow cover is an important process controlling the GPP–snow relationships in most regions of the TP, and the "moisture effect" plays an increasingly important role as drought levels increase. In contrast, the "growth period effect" directly on GPP is relatively weak. This study shed light on the importance of snow cover in regulating different seasonal GPP variations and significantly improves our insight into how vegetation carbon uptake responds to snow cover changes in the TP.

ACKNOWLEDGMENTS

This study was supported by the National Natural Science Foundation of China (Grant No. 42171307) and the "GeoX" Interdisciplinary Research Funds for the Frontiers Science Center for Critical Earth Material Cycling, Nanjing University.

CONFLICT OF INTEREST STATEMENT

The authors declare no conflicts of interest.

DATA AVAILABILITY STATEMENT

The daily snow cover extent product is available from https://cstr.cn/18406.11.Snow.tpdc.271381. The daily snow water equivalent product is available from http://www.doi.org/10.11922/sciencedb.j00076.00071. The Global LAnd Surface Satellite gross primary productivity data are available from http://www.glass.umd.edu/GPP/AVHRR/. Air temperature, precipitation, and shortwave radiation data are available from http://data.tpdc.ac.cn/en/data/8028b944-daaa-4511-8769-965612652c49/. Soil temperature data are available from https://doi.org/10.24381/cds.68d2bb30. The soil moisture data are available from https://www.gleam.eu.

REFERENCES

Bastos, A., R. Orth, M. Reichstein, P. Ciais, N. Viovy, S. Zaehle, P. Anthoni, et al. 2021. "Vulnerability of European Ecosystems to Two Compound Dry and Hot Summers in 2018 and 2019." *Earth System Dynamics* 12(4): 1015–35. https://doi.org/10.5194/esd-12-1015-2021.

Cao, R., Y. Chen, M. Shen, J. Chen, J. Zhou, C. Wang, and W. Yang. 2018. "A Simple Method to Improve the Quality of NDVI Time-Series Data by Integrating Spatiotemporal Information with the Savitzky–Golay Filter." *Remote Sensing of Environment* 217: 244–257. https://doi.org/10.1016/j.rse.2018.08.022.

Chen, H., Q. Zhu, C. Peng, N. Wu, Y. Wang, X. Fang, Y. Gao, et al. 2013. "The Impacts of Climate Change and Human Activities on Biogeochemical Cycles on the Qinghai-Tibetan Plateau." *Global Change Biology* 19(10): 2940–55. https://doi.org/10.1111/gcb.12277.

Chen, S., Y. Huang, and G. Wang. 2019. "Response of Vegetation Carbon Uptake to Snow-Induced Phenological and Physiological Changes across Temperate China." *Science of the Total Environment* 692: 188–200. https://doi.org/10.1016/j.scitotenv.2019.07.222.

Chen, S., T. Liang, H. Xie, Q. Feng, X. Huang, and H. Yu. 2014. "Interrelation among Climate Factors, Snow Cover, Grassland Vegetation, and Lake in the Nam Co Basin of the Tibetan Plateau." *Journal of Applied Remote Sensing* 8(1): 84694.

Chen, W., Y. Wu, N. Wu, and P. Luo. 2008. "Effect of Snow-Cover Duration on Plant Species Diversity of Alpine Meadows on the Eastern Qinghai-Tibetan Plateau." *Journal of Mountain Science* 5(4): 327–339. https://doi.org/10.1007/s11629-008-0182-0.

Chen, X., S. An, D. W. Inouye, and M. D. Schwartz. 2015. "Temperature and Snowfall Trigger Alpine Vegetation Green-Up on the World's Roof." *Global Change Biology* 21(10): 3635–46. https://doi.org/10.1111/gcb.12954.

Chimner, R. A., J. M. Welker, J. Morgan, D. LeCain, and J. Reeder. 2010. "Experimental Manipulations of Winter Snow and Summer Rain Influence Ecosystem Carbon Cycling in a Mixed-Grass Prairie, Wyoming, USA." *Ecohydrology* 3(3): 284–293. https://doi.org/10.1002/eco.106.

Choler, P. 2015. "Growth Response of Temperate Mountain Grasslands to Inter-Annual Variations in Snow Cover Duration." *Biogeosciences* 12(12): 3885–97. https://doi.org/10.5194/bg-12-3885-2015.

Cong, N., M. Shen, W. Yang, Z. Yang, G. Zhang, and S. Piao. 2017. "Varying Responses of Vegetation Activity to Climate Changes on the Tibetan Plateau Grassland." *International Journal of Biometeorology* 61(8): 1433–44. https://doi.org/10.1007/s00484-017-1321-5.

Dong, S., Z. Shang, J. Gao, and R. B. Boone. 2020. "Enhancing Sustainability of Grassland Ecosystems through Ecological Restoration and Grazing Management in an Era of Climate Change on Qinghai-Tibetan Plateau." *Agriculture, Ecosystems & Environment* 287: 106684. https://doi.org/10.1016/j.agee.2019.106684.

Galvagno, M., G. Wohlfahrt, E. Cremonese, M. Rossini, R. Colombo, G. Filippa, T. Julitta, et al. 2013. "Phenology and Carbon Dioxide Source/Sink Strength of a Subalpine Grassland in Response to an Exceptionally Short Snow Season." *Environmental Research Letters* 8(2): 25008. https://doi.org/10.1088/1748-9326/8/2/025008.

Guo, M., C. Wu, J. Peng, L. Lu, and S. Li. 2021. "Identifying Contributions of Climatic and Atmospheric Changes to Autumn Phenology over Mid-High Latitudes of Northern Hemisphere." *Global and Planetary Change* 197: 103396. https://doi.org/10.1016/j.gloplacha.2020.103396.

Hamed, K. H., and R. A. Rao. 1998. "A Modified Mann-Kendall Trend Test for Autocorrelated Data." *Journal of Hydrology* 204(1–4): 182–196. https://doi.org/10.1016/S0022-1694(97)00125-X.

Hao, X., G. Huang, T. Che, W. Ji, X. Sun, Q. Zhao, H. Zhao, J. Wang, H. Li, and Q. Yang. 2021. "The NIEER AVHRR Snow Cover Extent Product over China – A Long-Term Daily Snow Record for Regional Climate Research." *Earth System Science Data* 13(10): 4711–26. https://doi.org/10.5194/essd-13-4711-2021.

Hao, X., Q. Zhao, W. Ji, J. Wang, and H. Li. 2022. "A Dataset of Snow Cover Phenology in China Based on AVHRR from 1980 to 2020." *China Scientific Data* 7(3): 1–10. https://doi.org/10.11922/11-6035.ncdc.2021.0026.zh.

He, J., K. Yang, W. Tang, H. Lu, J. Qin, Y. Chen, and X. Li. 2020. "The First High-Resolution Meteorological Forcing Dataset for Land Process Studies over China." *Scientific Data* 7(1). https://doi.org/10.1038/s41597-020-0369-y.

Hou, X. 2019. *1: Million Vegetation Map of China* 113–124. Beijing: National Tibetan Plateau Data Center.

Hu, G., L. Zhao, R. Li, X. Wu, T. Wu, C. Xie, X. Zhu, and Y. Su. 2019. "Variations in Soil Temperature from 1980 to 2015 in Permafrost Regions on the Qinghai-Tibetan Plateau Based on Observed and Reanalysis Products." *Geoderma* 337: 893–905. https://doi.org/10.1016/j.geoderma.2018.10.044.

IPCC. 2021. *Climate Change 2021: The Physical Science Basis. Contribution of Working Group I to the Sixth Assessment Report of the Intergovernmental Panel on Climate Change*. Cambridge, UK and New York, NY: Cambridge University Press.

Ji, Z., and S. Kang. 2013. "Projection of Snow Cover Changes over China under RCP Scenarios." *Climate Dynamics* 41(3–4): 589–600. https://doi.org/10.1007/s00382-012-1473-2.

Jiang, L., J. Yang, L. Dai, X. Li, Y. Qiu, S. Wu, and Z. Li. 2020. *Snow Water Equivalent 25 km Daily Product in China from 1980 to 2020*. Lanzhou, China: National Cryosphere Desert Data Center. https://doi.org/10.12072/ncdc.I-SNOW.db0002.2020.

Jiang, L., J. Yang, C. Zhang, S. Wu, Z. Li, L. Dai, X. Li, and Y. Qiu. 2022. "Daily Snow Water Equivalent Product with SMMR, SSM/I and SSMIS from 1980 to 2020 over China." *Big Earth Data* 1-15: 420–434. https://doi.org/10.1080/20964471.2022.2032998.

Kang, Z., B. Qiu, Z. Xiang, Y. Liu, Z. Lin, and W. Guo. 2022. "Improving Simulations of Vegetation Dynamics over the Tibetan Plateau: Role of Atmospheric Forcing Data and Spatial Resolution." *Advances in Atmospheric Sciences* 39(7): 1115–32. https://doi.org/10.1007/s00376-022-1426-6.

Keenan, T. F., D. Y. Hollinger, G. Bohrer, D. Dragoni, J. W. Munger, H. P. Schmid, and A. D. Richardson. 2013. "Increase in Forest Water-Use Efficiency as Atmospheric Carbon Dioxide Concentrations Rise." *Nature* 499(7458): 324–27. https://doi.org/10.1038/nature12291.

Kelsey, K. C., S. H. Pedersen, A. J. Leffler, J. O. Sexton, M. Feng, and J. M. Welker. 2021. "Winter Snow and Spring Temperature Have Differential Effects on Vegetation Phenology and Productivity across Arctic Plant Communities." *Global Change Biology* 27(8): 1572–86. https://doi.org/10.1111/gcb.15505.

Knowles, J. F., L. R. Lestak, and N. P. Molotch. 2017. "On the Use of a Snow Aridity Index to Predict Remotely Sensed Forest Productivity in the Presence of Bark Beetle Disturbance." *Water Resources Research* 53(6): 4891–4906. https://doi.org/10.1002/2016WR019887.

Kuang, X., and J. J. Jiao. 2016. "Review on Climate Change on the Tibetan Plateau during the Last Half Century." *Journal of Geophysical Research: Atmospheres* 121(8): 3979–4007. https://doi.org/10.1002/2015JD024728.

Li, H., F. Liu, S. Zhang, C. Zhang, C. Zhang, W. Ma, and J. Luo. 2022. "Drying–Wetting Changes of Surface Soil Moisture and the Influencing Factors in Permafrost Regions of the Qinghai-Tibet Plateau, China." *Remote Sensing* 14(12): 2915. https://doi.org/10.3390/rs14122915.

Li, P., E. J. Sayer, Z. Jia, W. Liu, Y. Wu, S. Yang, C. Wang, et al. 2020. "Deepened Winter Snow Cover Enhances Net Ecosystem Exchange and Stabilizes Plant Community Composition and Productivity in a Temperate Grassland." *Global Change Biology* 26(5): 3015–27. https://doi.org/10.1111/gcb.15051.

Li, W., J. Wu, E. Bai, C. Jin, A. Wang, F. Yuan, and D. Guan. 2016. "Response of Terrestrial Carbon Dynamics to Snow Cover Change: A Meta-Analysis of Experimental Manipulation (II)." *Soil Biology and Biochemistry* 103: 388–393. https://doi.org/10.1016/j.soilbio.2016.09.017.

Liu, J., S. Li, Z. Ouyang, C. Tam, and X. Chen. 2008. "Ecological and Socioeconomic Effects of China's Policies for Ecosystem Services." *Proceedings of the National Academy of Sciences of the United States of America* 105(28): 9477–82. https://doi.org/10.1073/pnas.0706436105.

Luo, Z., W. Feng, Y. Luo, J. Baldock, and E. Wang. 2017. "Soil Organic Carbon Dynamics Jointly Controlled by Climate, Carbon Inputs, Soil Properties and Soil Carbon Fractions." *Global Change Biology* 23(10): 4430–39. https://doi.org/10.1111/gcb.13767.

Ma, J., X. Xiao, R. Miao, Y. Li, B. Chen, Y. Zhang, and B. Zhao. 2019. "Trends and Controls of Terrestrial Gross Primary Productivity of China during 2000-2016." *Environmental Research Letters* 14(8): 84032. https://doi.org/10.1088/1748-9326/ab31e4.

Magnani, A., D. Viglietti, D. Godone, M. W. Williams, R. Balestrini, and M. Freppaz. 2017. "Interannual Variability of Soil N and C Forms in Response to Snow-Cover Duration and Pedoclimatic Conditions in Alpine Tundra, Northwest Italy." *Arctic, Antarctic, and Alpine Research* 49(2): 227–242. https://doi.org/10.1657/AAAR0016-037.

Martens, B., D. G. Miralles, H. Lievens, R. van der Schalie, R. A. M. de Jeu, D. Fernández-Prieto, H. E. Beck, W. A. Dorigo, and N. E. C. Verhoest. 2017. "GLEAM v3: Satellite-Based Land Evaporation and Root-Zone Soil Moisture." *Geoscientific Model Development* 10(5): 1903–25. https://doi.org/10.5194/gmd-10-1903-2017.

Muñoz-Sabater, J., E. Dutra, A. Agustí-Panareda, C. Albergel, G. Arduini, G. Balsamo, S. Boussetta, et al. 2021. "ERA5-Land: A State-of-the-Art Global Reanalysis Dataset for Land Applications." *Earth System Science Data* 13(9): 4349–83. https://doi.org/10.5194/essd-13-4349-2021.

Notarnicola, C. 2020. "Hotspots of Snow Cover Changes in Global Mountain Regions over 2000–2018." *Remote Sensing of Environment* 243: 111781. https://doi.org/10.1016/j.rse.2020.111781.

Peng, S., S. Piao, P. Ciais, J. Fang, and X. Wang. 2010. "Change in Winter Snow Depth and Its Impacts on Vegetation in China."

Global Change Biology 16: 3004–13. https://doi.org/10.1111/j.1365-2486.2010.02210.x.

Peng, S., S. Piao, P. Ciais, P. Friedlingstein, L. Zhou, and T. Wang. 2013. "Change in Snow Phenology and Its Potential Feedback to Temperature in the Northern Hemisphere over the Last Three Decades." *Environmental Research Letters* 8(1): 14008.

Piao, S., Q. Liu, A. Chen, I. A. Janssens, Y. Fu, J. Dai, L. Liu, X. Lian, M. Shen, and X. Zhu. 2019. "Plant Phenology and Global Climate Change: Current Progresses and Challenges." *Global Change Biology* 25(6): 1922–40. https://doi.org/10.1111/gcb.14619.

Piao, S., K. Tan, H. Nan, P. Ciais, J. Fang, T. Wang, N. Vuichard, and B. Zhu. 2012. "Impacts of Climate and CO_2 Changes on the Vegetation Growth and Carbon Balance of Qinghai–Tibetan Grasslands over the past Five Decades." *Global and Planetary Change* 98-99: 73–80. https://doi.org/10.1016/j.gloplacha.2012.08.009.

Pulliainen, J., M. Aurela, T. Laurila, T. Aalto, M. Takala, M. Salminen, M. Kulmala, et al. 2017. "Early Snowmelt Significantly Enhances Boreal Springtime Carbon Uptake." *Proceedings of the National Academy of Sciences of the United States of America* 114(42): 11081–86. https://doi.org/10.1073/pnas.1707889114.

Qi, Y., H. Wang, X. Ma, J. Zhang, and R. Yang. 2021. "Relationship between Vegetation Phenology and Snow Cover Changes during 2001–2018 in the Qilian Mountains." *Ecological Indicators* 133: 108351. https://doi.org/10.1016/j.ecolind.2021.108351.

Qin, Y., T. Wu, X. Wu, R. Li, C. Xie, Y. Qiao, G. Hu, X. Zhu, W. Wang, and W. Shang. 2017. "Assessment of Reanalysis Soil Moisture Products in the Permafrost Regions of the Central of the Qinghai-Tibet Plateau." *Hydrological Processes* 31(26): 4647–59. https://doi.org/10.1002/hyp.11383.

Qiu, B., W. Li, X. Wang, L. Shang, C. Song, W. Guo, and Y. Zhang. 2019. "Satellite-Observed Solar-Induced Chlorophyll Fluorescence Reveals Higher Sensitivity of Alpine Ecosystems to Snow Cover on the Tibetan Plateau." *Agricultural and Forest Meteorology* 271: 126–134. https://doi.org/10.1016/j.agrformet.2019.02.045.

Sa, C., F. Meng, M. Luo, C. Li, M. Wang, S. Adiya, and Y. Bao. 2021. "Spatiotemporal Variation in Snow Cover and Its Effects on Grassland Phenology on the Mongolian Plateau." *Journal of Arid Land* 13(4): 332–349. https://doi.org/10.1007/s40333-021-0056-7.

Sanchez, G. 2013. *PLS Path Modeling with R*. Berkeley, CA: Trowchez Editions, 383 pp.

Scholz, K., A. Hammerle, E. Hiltbrunner, and G. Wohlfahrt. 2018. "Analyzing the Effects of Growing Season Length on the Net Ecosystem Production of an Alpine Grassland Using Model–Data Fusion." *Ecosystems* 21(5): 982–999. https://doi.org/10.1007/s10021-017-0201-5.

Sen, P. K. 1968. "Estimates of the Regression Coefficient Based on Kendall's Tau." *Journal of the American Statistical Association* 63(324): 1379–89.

Shen, M., S. Wang, N. Jiang, J. Sun, R. Cao, X. Ling, B. Fang, et al. 2022. "Plant Phenology Changes and Drivers on the Qinghai–Tibetan Plateau." *Nature Reviews Earth & Environment* 3: 633–651. https://doi.org/10.1038/s43017-022-00317-5.

Shen, S. S. P., R. Yao, J. Ngo, A. M. Basist, N. Thomas, and T. Yao. 2015. "Characteristics of the Tibetan Plateau Snow Cover Variations Based on Daily Data during 1997–2011." *Theoretical and Applied Climatology* 120(3–4): 445–453. https://doi.org/10.1007/s00704-014-1185-0.

Sherwood, J. A., D. M. Debinski, P. C. Caragea, and M. J. Germino. 2017. "Effects of Experimentally Reduced Snowpack and Passive Warming on Montane Meadow Plant Phenology and Floral Resources." *Ecosphere* 8(3): e1745. https://doi.org/10.1002/ecs2.1745.

Smith, T., and B. Bookhagen. 2018. "Changes in Seasonal Snow Water Equivalent Distribution in High Mountain Asia (1987 to 2009)." *Science Advances* 4(1): e1701550. https://doi.org/10.1126/sciadv.1701550.

Sun, Y., T. Zhang, Y. Liu, W. Zhao, and X. Huang. 2020. "Assessing Snow Phenology over the Large Part of Eurasia Using Satellite Observations from 2000 to 2016." *Remote Sensing* 12(12): 2060. https://doi.org/10.3390/rs12122060.

Tang, Z., G. Deng, G. Hu, H. Zhang, H. Pan, and G. Sang. 2022. "Satellite Observed Spatiotemporal Variability of Snow Cover and Snow Phenology over High Mountain Asia from 2002 to 2021." *Journal of Hydrology* 613: 128438. https://doi.org/10.1016/j.jhydrol.2022.128438.

Tomaszewska, M. A., L. H. Nguyen, and G. M. Henebry. 2020. "Land Surface Phenology in the Highland Pastures of Montane Central Asia: Interactions with Snow Cover Seasonality and Terrain Characteristics." *Remote Sensing of Environment* 240: 111675. https://doi.org/10.1016/j.rse.2020.111675.

Wagg, C., S. F. Bender, F. Widmer, and M. G. A. van der Heijden. 2014. "Soil Biodiversity and Soil Community Composition Determine Ecosystem Multifunctionality." *Proceedings of the National Academy of Sciences of the United States of America* 111(14): 5266–70. https://doi.org/10.1073/pnas.1320054111.

Wan, Y., Q. Gao, Y. Li, X. Qin, Ganjurjav, W. Zhang, X. Ma, and S. Liu. 2014. "Change of Snow Cover and Its Impact on Alpine Vegetation in the Source Regions of Large Rivers on the Qinghai-Tibetan Plateau, China." *Arctic, Antarctic, and Alpine Research* 46(3): 632–644. https://doi.org/10.1657/1938-4246-46.3.632.

Wang, J., and D. Liu. 2022. "Vegetation Green-Up Date Is More Sensitive to Permafrost Degradation than Climate Change in Spring across the Northern Permafrost Region." *Global Change Biology* 28(4): 1569–82. https://doi.org/10.1111/gcb.16011.

Wang, K., L. Zhang, Y. Qiu, L. Ji, F. Tian, C. Wang, and Z. Wang. 2015. "Snow Effects on Alpine Vegetation in the Qinghai-Tibetan Plateau." *International Journal of Digital Earth* 8(1): 58–75. https://doi.org/10.1080/17538947.2013.848946.

Wang, S., X. Wang, G. Chen, Q. Yang, B. Wang, Y. Ma, and M. Shen. 2017. "Complex Responses of Spring Alpine Vegetation Phenology to Snow Cover Dynamics over the Tibetan Plateau, China." *Science of the Total Environment* 593-594: 449–461. https://doi.org/10.1016/j.scitotenv.2017.03.187.

Wang, T., Y. Zhao, C. Xu, P. Ciais, D. Liu, H. Yang, S. Piao, and T. Yao. 2021. "Atmospheric Dynamic Constraints on Tibetan Plateau Freshwater under Paris Climate Targets." *Nature Climate Change* 11(3): 219–225. https://doi.org/10.1038/s41558-020-00974-8.

Wang, X., T. Wang, H. Guo, D. Liu, Y. Zhao, T. Zhang, Q. Liu, and S. Piao. 2018. "Disentangling the Mechanisms Behind Winter

Snow Impact on Vegetation Activity in Northern Ecosystems." *Global Change Biology* 24(4): 1651–62. https://doi.org/10.1111/gcb.13930.

Wang, X., C. Wu, D. Peng, A. Gonsamo, and Z. Liu. 2018. "Snow Cover Phenology Affects Alpine Vegetation Growth Dynamics on the Tibetan Plateau: Satellite Observed Evidence, Impacts of Different Biomes, and Climate Drivers." *Agricultural and Forest Meteorology* 256-257: 61–74. https://doi.org/10.1016/j.agrformet.2018.03.004.

Wang, X., J. Xiao, X. Li, G. Cheng, M. Ma, G. Zhu, M. Altaf Arain, T. Andrew Black, and R. S. Jassal. 2019. "No Trends in Spring and Autumn Phenology during the Global Warming Hiatus." *Nature Communications* 10(1): 2389. https://doi.org/10.1038/s41467-019-10235-8.

Wang, Y., B. Fu, Y. Liu, Y. Li, X. Feng, and S. Wang. 2021. "Response of Vegetation to Drought in the Tibetan Plateau: Elevation Differentiation and the Dominant Factors." *Agricultural and Forest Meteorology* 306: 108468. https://doi.org/10.1016/j.agrformet.2021.108468.

Wei, D., Y. Qi, Y. Ma, X. Wang, W. Ma, T. Gao, L. Huang, H. Zhao, J. Zhang, and X. Wang. 2021. "Plant Uptake of CO_2 Outpaces Losses from Permafrost and Plant Respiration on the Tibetan Plateau." *Proceedings of the National Academy of Sciences of the United States of America* 118(33): e2015283118. https://doi.org/10.1073/pnas.2015283118.

Wei, Z., and W. Dong. 2015. "Assessment of Simulations of Snow Depth in the Qinghai-Tibetan Plateau Using CMIP5 Multi-Models." *Arctic, Antarctic, and Alpine Research* 47(4): 525–611. https://doi.org/10.1657/AAAR0014-050.

Wetzels, M., G. Odekerken-Schröder, and C. Van Oppen. 2009. "Using PLS Path Modeling for Assessing Hierarchical Construct Models: Guidelines and Empirical Illustration." *MIS Quarterly* 33: 177–195.

Wipf, S., and C. Rixen. 2010. "A Review of Snow Manipulation Experiments in Arctic and Alpine Tundra Ecosystems." *Polar Research* 29(1): 95–109.

Wold, S. 1995. "PLS for Multivariate Linear Modeling." *Chemometric Methods in Molecular Design* 58: 195–218.

Wu, C., J. M. Chen, A. Gonsamo, D. T. Price, T. A. Black, and W. A. Kurz. 2012. "Interannual Variability of Net Carbon Exchange Is Related to the Lag between the End-Dates of Net Carbon Uptake and Photosynthesis: Evidence from Long Records at Two Contrasting Forest Stands." *Agricultural and Forest Meteorology* 164: 29–38. https://doi.org/10.1016/j.agrformet.2012.05.002.

Wu, X., X. Li, H. Liu, P. Ciais, Y. Li, C. Xu, F. Babst, et al. 2018. "Uneven Winter Snow Influence on Tree Growth across Temperate China." *Global Change Biology* 25(1): 144–154. https://doi.org/10.1111/gcb.14464.

Xie, J., F. Hüsler, R. de Jong, B. Chimani, S. Asam, Y. Sun, M. E. Schaepman, and M. Kneubühler. 2021. "Spring Temperature and Snow Cover Climatology Drive the Advanced Springtime Phenology (1991–2014) in the European Alps." *Journal of Geophysical Research: Biogeosciences* 126(3): e2020JG006150. https://doi.org/10.1029/2020JG006150.

Xu, C., N. G. McDowell, R. A. Fisher, L. Wei, S. Sevanto, B. O. Christoffersen, E. Weng, and R. S. Middleton. 2019. "Increasing Impacts of Extreme Droughts on Vegetation Productivity under Climate Change." *Nature Climate Change* 9(12): 948–953. https://doi.org/10.1038/s41558-019-0630-6.

Xu, W., L. Ma, M. Ma, H. Zhang, and W. Yuan. 2017. "Spatial–Temporal Variability of Snow Cover and Depth in the Qinghai–Tibetan Plateau." *Journal of Climate* 30(4): 1521–33. https://doi.org/10.1175/JCLI-D-15-0732.1.

Yang, S., R. Li, T. Wu, G. Hu, Y. Xiao, Y. Du, X. Zhu, et al. 2020. "Evaluation of Reanalysis Soil Temperature and Soil Moisture Products in Permafrost Regions on the Qinghai-Tibetan Plateau." *Geoderma* 377: 114583. https://doi.org/10.1016/j.geoderma.2020.114583.

Yano, Y., E. N. J. Brookshire, J. Holsinger, and T. Weaver. 2015. "Long-Term Snowpack Manipulation Promotes Large Loss of Bioavailable Nitrogen and Phosphorus in a Subalpine Grassland." *Biogeochemistry* 124(1–3): 319–333. https://doi.org/10.1007/s10533-015-0100-9.

Yao, T., Y. Xue, D. Chen, F. Chen, L. Thompson, P. Cui, T. Koike, et al. 2019. "Recent Third Pole's Rapid Warming Accompanies Cryospheric Melt and Water Cycle Intensification and Interactions between Monsoon and Environment: Multi-Disciplinary Approach with Observation, Modeling and Analysis." *Bulletin of the American Meteorological Society* 100: 423–434. https://doi.org/10.1175/BAMS-D-17-0057.1.

You, Q., F. Wu, H. Wang, Z. Jiang, N. Pepin, and S. Kang. 2020. "Projected Changes in Snow Water Equivalent over the Tibetan Plateau under Global Warming of 1.5° and 2°C." *Journal of Climate* 33(12): 5141–54. https://doi.org/10.1175/JCLI-D-19-0719.1.

Yu, H., E. Luedeling, and J. Xu. 2010. "Winter and Spring Warming Result in Delayed Spring Phenology on the Tibetan Plateau." *Proceedings of the National Academy of Sciences of the United States of America* 107(51): 22151–56. https://doi.org/10.1073/pnas.1012490107.

Yu, T., R. Sun, Z. Xiao, Q. Zhang, G. Liu, T. Cui, and J. Wang. 2018. "Estimation of Global Vegetation Productivity from Global LAnd Surface Satellite Data." *Remote Sensing* 10(2): 327. https://doi.org/10.3390/rs10020327.

Yuan, W., S. Liu, G. Yu, J. Bonnefond, J. Chen, K. Davis, A. R. Desai, et al. 2010. "Global Estimates of Evapotranspiration and Gross Primary Production Based on MODIS and Global Meteorology Data." *Remote Sensing of Environment* 114(7): 1416–31. https://doi.org/10.1016/j.rse.2010.01.022.

Zhang, G., H. Xie, T. Yao, T. Liang, and S. Kang. 2012. "Snow Cover Dynamics of Four Lake Basins over Tibetan Plateau Using Time Series MODIS Data (2001–2010)." *Water Resources Research* 48(10). https://doi.org/10.1029/2012WR011971.

Zhang, Q., D. Kong, P. Shi, V. P. Singh, and P. Sun. 2018. "Vegetation Phenology on the Qinghai-Tibetan Plateau and Its Response to Climate Change (1982–2013)." *Agricultural and Forest Meteorology* 248: 408–417. https://doi.org/10.1016/j.agrformet.2017.10.026.

Zhang, X., M. A. Friedl, C. B. Schaaf, A. H. Strahler, J. C. Hodges, F. Gao, B. C. Reed, and A. Huete. 2003. "Monitoring Vegetation Phenology Using MODIS." *Remote Sensing of Environment* 84(3): 471–75.

Zhang, Y., R. Commane, S. Zhou, A. P. Williams, and P. Gentine. 2020. "Light Limitation Regulates the Response of Autumn Terrestrial Carbon Uptake to Warming." *Nature Climate Change* 10(8): 739–743. https://doi.org/10.1038/s41558-020-0806-0.

Zhang, Y., and N. Ma. 2018. "Spatiotemporal Variability of Snow Cover and Snow Water Equivalent in the Last Three Decades over Eurasia." *Journal of Hydrology* 559: 238–251. https://doi.org/10.1016/j.jhydrol.2018.02.031.

Zhumanova, M., C. Mönnig, C. Hergarten, D. Darr, and N. Wrage-Mönnig. 2018. "Assessment of Vegetation Degradation in Mountainous Pastures of the Western Tien-Shan, Kyrgyzstan, Using eMODIS NDVI." *Ecological Indicators* 95: 527–543. https://doi.org/10.1016/j.ecolind.2018.07.060.

How to cite this article: Liu, Hao, Pengfeng Xiao, Xueliang Zhang, and Youlv Wu. 2023. "Increased Snow Cover Enhances Gross Primary Productivity in Cold and Dry Regions of the Tibetan Plateau." *Ecosphere* 14(9): e4656. https://doi.org/10.1002/ecs2.4656